

Performance Improvement of Sensorless Direct Field Oriented Induction Motor Drive with Sliding Mode and Fuzzy Sliding Mode Controllers

Presented by

Swetananda Jena

M.Tech(R)

Roll No.-609EE101

Under the guidance of

Prof. K. B. Mohanty

Associate Professor



Department of Electrical Engineering

National Institute of Technology, Rourkela-769008

CERTIFICATE

This is to certify that the work in this thesis entitled “Performance Improvement of Sensorless Direct Field Oriented Induction Motor Drive with Sliding Mode and Fuzzy Sliding Mode Controllers”, submitted by Mrs. Swetananda Jena, for the award of degree for Master of Technology in ‘Power Control and Drives’ during the period from July 2009 to July 2012 in the department of electrical engineering, National Institute of Technology,, Rourkela and is an authentic work by her under my supervision and guidance.

To the best of my knowledge and belief, this work has not been submitted to any degree or diploma.

Place:

Prof. K. B. Mohanty

Date:

Dept. of Electrical Engg.

National Institute of Technology

Rourkela-769008

Orissa

AKNOWLEDGEMENTS

I feel a great pleasure in expressing my sincere thanks to my supervisor Prof. K. B. Mohanty for his encouragement guidance and valuable suggestion throughout the study of power electronics and machine drives. I am grateful for his generous support and constructive engagement during the course of my stay at National Institute Technology. His constant help, supervision and inspiration led me to do this work, which involves the concept of control system, application, power electronics as well as electrical machines.

I express my heartfelt gratitude to Prof B. D. Subudhi for his motivation during the research work. His ideas and suggestions helped me to carry out the research work.

I sincerely thank to Prof. A. K, Panda for providing me all his lab facilities and encouragement which help completing my research work.

I am grateful to Prof. K. B. Mohanty and Prof. A. K. Panda for their guidance and support over the coursework to provide a strong background for my studies and research thereafter.

I also thank to the laboratory staff and administrative staff of Electrical Engineering department for their timely help and co-operation during the research work.

Most of all, I would like to thank everyone in my family due to their great trust, encouragement and un-interpreted emotional support.

Date:

Swetananda Jena

Place:

M.Tech(R),

Power Control & Drives

ABSTRACT

For high performance, variable speed applications, the Induction Motors are used widely due to its low cost, low maintenance, requirement, robustness and reliability, thus replacing the DC motor drives. For wide range of speed applications and fast torque response, IMs perform satisfactory with the vector control strategy. Because of the higher order unmodeled system dynamics and different machine parameters such as rotor speed, stator and rotor resistance variation and load torque variation, different nonlinear controllers are used to increase its robustness and to make the system stable. However, the use of linear controller does not give satisfactory performance due to the above causes.

IM is mathematically to get an approximate idea of the actual plant model. The vector control of IM is implemented by using different controllers such as P-I, sliding mode controller and a hybrid controller such as fuzzy sliding mode controller. To make the system to remain in steady-state, P-I controller is used and due to the more sensitive action of the derivative controller, it is not used.

The sliding mode controller is designed for robust control of IM. Under different adverse condition, its performance is satisfactory. But, the main disadvantage of sliding mode controller is the chattering problem that can be reduced by taking necessary steps. The disadvantage of the sliding mode controller is eliminated by a hybrid controller such as fuzzy sliding mode controller.

To make the system sensorless, we go for rotor speed estimation using direct synthesis of state equation, as the closed loop control requires the speed sensor. By using speed sensor, the IM becomes more costly and less reliable and increased maintenance cost. The different simulation results are observed and studied and the analysis of the different simulated results are presented.

LIST OF SYMBOLS

V_{ds}, V_{dr}	d-axis stator and rotor voltages
V_{qs}, V_{qr}	q-axis stator and rotor voltages
R_s, R_r	Stator and rotor resistances
L_s, L_r	Leakage inductance per phase of stator and rotor referred to stator
L_m	Magnetizing inductance per phase referred to stator
i_{ds}, i_{qs}	d- and q-axis stator currents
i_{dr}, i_{qr}	d- and q-axis rotor currents
i_s, i_r	Stator and rotor phase currents
Ψ_{ds}, Ψ_{qs}	Stator d- and q-axis fluxes
Ψ_{dr}, Ψ_{qr}	Rotor d- and q-axis fluxes
Ψ_{dr}^*, Ψ_{qr}^*	Rotor d- and q-axis reference flux
ω_e	Speed of the reference frame in rad/s
ω_r	Rotor electrical speed in rad/s
ω_m	Rotor mechanical speed in rad/s
ω_{sl}	Electrical slip speed in rad/s
ω_n	Natural frequency of the system in radian
T_e	Electromagnetic torque developed in N.m
T_e^*	Reference torque in N.m

T_l	Load torque in N.m
P	No. of poles
J	Moment of inertia in kg.m ²
β	Co-efficient of viscous friction in N.m.s/rad
σ	Leakage co-efficient
p	Rate of change of derivative
a_1, a_2, a_3, a_4, a_5	Induction motor modeling parameters
u_1, u_2	Control input voltages for speed and flux controller
$G_{(s)}$	Transfer function
$K_{p\psi}, K_{i\psi}$	Proportional and integral constants of flux controller
K_{pT}, K_{iT}	Proportional and integral constants of Torque controller
τ_{T_e}	Time constant
K_T	Torque constant of the motor
D_1, D_2	Total disturbance in speed and flux controller
λ	Bandwidth of the sliding mode controller
n	Order of the system
e	Tracking error vector
θ_e	Rotor angle

LIST OF TABLES

Table 1	Fuzzy Rules	65
Table 2	Performance comparison of the controllers for a step change in rotor speed from 1445rpm to 1734rpm	83
Table 3	Performance comparison of the controllers for a step change in load torque from 0 to 24Nm	83
Table 4	Performance comparison of the controllers for flux weakening mode	83
Table 5	Parameters of the Induction Motor	87
Table 6	Values of the parameters used in the induction motor model	87

LIST OF FIGURES

Figure 2.1 Block diagram of electrical subsystem.....	26
Figure 2.2 Block diagram of mechanical subsystem	29
Figure 2.3 Block Diagram for Vector Control of Induction Motor	31
Figure 2.4 Simulation responses for step change in reference rotor speed.....	32
Figure 2.5 Simulation responses for Trapezoidal change in reference rotor speed	33
Figure 2.6 Simulation responses for trapezoidal change in reference speed during flux weakening mode	34-35
Figure 2.7 Simulation responses for step change in load torque.....	35-36
Figure 3.1 Simulation responses for step change in reference speed.....	51-52
Figure 3.2 Simulation responses for trapezoidal change in reference speed during flux weakening mode	53-54
Figure 3.3 Simulation responses for step change in reference speed during flux weakening mode.....	55
Figure 3.4 Simulation responses during change in load torque	56-57
Figure 3.5 Simulation responses during Change of motor parameter variation.....	57-58
Figure 4.1 Block Diagram of Fuzzy Sliding Mode Controller.....	63
Figure 4.2 Membership functions for the normalized inputs.....	67
Figure 4.3 Membership functions for the normalized outputs.....	67
Figure 4.4 Simulation responses for step change in reference rotor speed.....	70
Figure 4.5 Simulation responses for Trapezoidal change in reference rotor speed.....	71-72
Figure 4.6 Simulation responses for step change in reference speed during flux weakening mode.....	72-73
Figure 4.7 Simulation responses during change in load torque.....	73-74
Figure 4.8 Simulation responses due to parameter variations.....	75-76

CONTENTS

1. INTRODUCTION	13
1.1 General	13
1.1.1 Scalar Control	13
1.1.2 Vector Control.....	13
1.2 Controller Design	14
1.3 Speed Estimation Techniques	15
1.4 Control Schemes.....	16
1.4.1 P-I Controller	16
1.4.2 Sliding Mode Controller (SMC)	16
1.4.3 Fuzzy Sliding Mode Controller (FSMC)	16
2. INDUCTION MACHINE MODELING AND DESIGN OF P-I CONTROLLERS.....	20
2.1 Introduction.....	20
2.2 Induction Motor Modeling.....	20
2.3 Design of P-I controllers	24
2.3.1 Electrical Subsystem	25
2.3.2 Mechanical subsystem	28
2.4 Simulation Results and Discussions	30
2.5 Conclusion	36
3. DESIGN OF SLIDING MODE CONTROLLERS.....	39
3.1 Introduction.....	39
3.2 Sliding mode controller.....	39
3.2.1 Control Law for Speed and Flux Control.....	44
3.2.2 Design of the controller's gains	46
3.3 Rotor Speed Estimation	49

3.4 Simulation Results and Discussions	50
3.5 Conclusion	58
4. DESIGN OF FUZZY SLIDING MODE CONTROLLERS.....	61
4.1 Introduction.....	61
4.2 Qualitative Aspects of Fuzzy Rule Design	61
4.3 Design of Fuzzy Logic Controller	61
4.4 Design of Fuzzy Sliding Mode controller.....	61
4.5 Simulation Results and Discussions	70
4.6 Conclusion	76
5. CONCLUSION.....	79
5.1 Assessment of the work	79
5.2 Comparison of the responses of all the controllers.....	80
5.3 Scope for the future work.....	84
References.....	85-86
Specifications and parameters of the machine.....	87

CHAPTER – 1
INTRODUCTION

1. INTRODUCTION

1.1 General

With the developments in power electronics, variable speed applications of both DC and AC machines gained momentum. The DC drives use thyristor controlled rectifiers to provide high performance torque, speed and flux control. The variable speed induction motor drives use mainly dc-ac inverters with pulse width modulation (pwm) techniques to generate a poly-phase supply of a given frequency. Most of the industrial applications that require good torque, speed or position control traditionally use DC motors. But, the advantages of induction motors are clear in terms of robustness, high torque-to-weight ratio, higher reliability, ability to operate in hazardous environment and price. After the development and implementation of field oriented control of induction motors, they became able to compete with DC machines in high performance applications. The induction motor dynamics can be compared to that of a DC motor with fast transient response if the flux producing and torque producing components of the stator current can be controlled independently which means it is possible to control the amplitude and phase angle independently.

1.1.1 Scalar Control

It is a non-vector control scheme featured by only magnitude control. It is a very simple method of speed control for motor drives. The speed of the motor can be controlled by changing the magnitude of voltage or frequency of the induction motor. The air gap flux can be controlled by the voltage and the frequency and is used to control the torque. As the flux and torque are both functions of frequency and voltage respectively, so, there exist the coupling effect between the flux and torque, which degrades the performance of the scalar control. The dynamic performance of the scalar control can be used for small variation of motor speed and load, it. But, for high performance drives, its performance is not satisfactory.

1.1.2 Vector Control

The principle of field orientation [1]-[3] for high performance control of machines was developed in Germany in the late sixties and earlier seventies. Its principle is that the machine

flux and torque are controlled independently, in a similar fashion to a separately excited DC machine. The stator current is resolved into two orthogonal components, one in the direction of flux linkage, representing magnetizing current or flux component of current and the other perpendicular to it, representing the torque component of current. Both the components are controlled independently. The two possible methods for achieving field orientation are; direct flux orientation where the field orientation is achieved by direct measurement or estimation of the flux, and indirect field orientation where the field orientation is achieved by imposing slip frequency derived from the rotor dynamic equations. The field orientation with respect to the rotor flux alone gives a natural decoupling between two components, fast torque response and stability; whereas the stator and air-gap flux decoupling control methods give nonlinear torque-slip characteristic with limited starting torque capability, though these methods are having ease of flux computation.

The advantages and disadvantages of the field orientation with different orientation schemes were studied in the literature [4, 5], from which it was concluded that the rotor flux oriented control only gives the natural decoupling of flux and torque [5], fast torque response and stability [6], whereas the stator and air gap flux orientation give nonlinear torque-slip characteristics and limited starting torque capability. The study and design procedures of P-I controllers are given in [2]. The hysteresis controller has fast transient response and the magnitude of the error of controlled parameter is bounded, whereas in steady-state, the ripple is high. In P-I controllers, the effective gains are decreased as a function of the increased motor speed [6] which can be overcome by a synchronous P-I regulator. With P-I controllers, the steady-state error becomes zero.

1.2 Controller Design

The field oriented control decouples the torque and flux producing components of stator currents of an induction machine and make them orthogonal like that of a separately excited dc machine, where the commutator does the above purpose. The vector control method uses an induction motor model and feedback of the rotor speed and produces the decoupled flux and torque producing components of stator phase current through controllers.

The study and design procedures of P-I controllers are given in [2]. The hysteresis controller has fast transient response and the magnitude of the error of controlled parameter is

bounded, whereas in steady-state, the ripple is high. In P-I controllers, the effective gains are decreased as a function of the increased motor speed [8] which can be overcome by a synchronous P-I regulator. With P-I controllers, the steady-state error becomes zero.

1.3 Speed Estimation Techniques

The speed estimation is an important aspect of the field oriented control in the recent years. The induction motor drives without mechanical speed sensors have low cost and size and high reliability. There are many techniques for sensorless closed-loop speed control of an induction motor. In the indirect field-oriented control of induction motor, slip speed estimation is based on the measured or estimated rotor speed to calculate the synchronous speed of the motor, whereas in the direct field oriented control, the synchronous speed is computed with the aid of a flux estimator.

Many speed estimation algorithms and speed sensor less control schemes have been developed. Some of the approaches are:-

- ❖ Speed estimation by the parameter identification approach [16, 17, and 18]. But, the parameter variation affects the performance of the estimator resulting in deterioration of the performance [19].
- ❖ Kalman filter algorithm and its extensions are robust and efficient observers for linear and nonlinear systems. An extended Kalman filter is used in [12] for speed estimation of vector controlled induction motor drives.
- ❖ Many Model Reference Adaptive Systems (MRAS) based speed sensorless schemes have been studied in [20, 21].
- ❖ Machine saliency based on fundamental or high frequency signal injection method has also been used for rotor position and speed estimation techniques. This technique is insensitive to actual motor parameter variations, but at low and zero speed operation, the performance is not much appreciable. Also, it causes torque ripples and vibration and noise at high frequency signal injection [8].

1.4 Control Schemes

1.4.1 P-I Controller

The P-I controllers are widely used in industries for high performances of electric drives. The ordinary method for the selection of the P-I gains is by trial and error method. Also, it makes the steady-state error zero. But, choosing improper P-I gains may affect the system variables. So, they need to be designed properly. The P-I gains can be designed by modulus optimum method. The pole-zero cancellation technique is another method to design the gains. The P-I controllers cause the overshoot and undershoot of the system response. The gains can be optimized by different optimization techniques such as Genetic Algorithm (GA) and Particle Swarm Optimization (PSO). In high performance ac drives, P-I controllers fails to achieve perfect control over the speed and load variation, in the presence of external and internal disturbance in the system and parameter variations. So, the efficiency, reliability and performance of the ac drives may deteriorate, which leads to employment of other nonlinear and hybrid controllers.

1.4.2 Sliding Mode Controller (SMC)

Sliding mode control is a nonlinear control technique that makes the system robust to parameter variations, modeling inaccuracies, external disturbances. This controller provides stability, faster dynamics and satisfactory performance for a higher order nonlinear system like induction motor drive. SMC is computationally simple compared to the adaptive controllers. These advantages of SMC can be employed in position and speed control of an ac servo system. An SMC design method based on synchronously rotating reference frame is presented in [22]. The chattering effect is the main disadvantage of the SMC. This chattering effect can be eliminated by introducing a saturation (sat) function. Here, the SMC technique is utilized for a direct field oriented induction motor drive to get a robust nonlinear control law to model uncertainties, inaccuracies and many other aspects.

1.4.3 Fuzzy Sliding Mode Controller (FSMC)

Fuzzy sliding mode controller is a hybrid controller that combines the fuzzy logic and the sliding mode technique. Irrespective of the robustness of the sliding mode controller against any uncertainties and disturbances, it is associated with the chattering problem and high controller

gains. So, reduction of this chattering effect can be achieved by a hybrid controller like FSMC that can give chattering free response without sacrificing the robustness of the system. The FSMC combines the advantages of sliding mode controller and fuzzy logic controller and reflects it in the system performance. The FLC is a simple rule based control system where the rules for this are decided by the user. Here, the inputs and the outputs, both are in the form of linguistic or fuzzy variables. The fuzzy sliding mode hybrid controller has the ability to account for modeling imprecision and external disturbances while the fuzzy logic controller provides better damping and reduced chattering.

1.5 Objectives

The vector controlled induction motor drive is associated with the nonlinearities due to the higher order differential equation in the mathematical modeling of the induction motor. The induction motor drive is linearized and decoupled into two subsystems i.e. electrical and mechanical. The induction motor drive is simulated with the P-I controllers. For sensorless control, many speed estimation techniques has been adopted to avoid measurement noise and to decrease the maintenance cost. Direct synthesis of state equations method is used in this thesis for robust and accurate rotor speed estimation. The motor parameter variations cause the disturbances in the system responses. The P-I controller gains require regular tuning with the parameter variations. To improve the dynamic and steady-state performance of the system, efforts are being made. For the high performance control of induction motor drive, sliding mode control is used for robust control against parameter variations, noise, machine unmodeled dynamics and load disturbances. But, due to the chattering problem associated with it, different controllers are being adopted. Fuzzy logic controller is one of the controllers which give better performance out of the modern simple controllers for industrial applications. Use of hybrid controller such as fuzzy sliding mode controller overcomes the disadvantages of sliding mode controller and therefore is more robust. So, the fuzzy sliding mode controller is a preferred one for the purpose of industrial application.

1.6 Organization of the Thesis

The organization of the thesis is given below. The vector control of induction motor is introduced in chapter 1. The design of the speed and flux controller as well as the speed

estimation techniques are studied in the literature survey. The flux estimation using observer is also studied. The design of both linear as well as nonlinear controllers such as P-I, sliding mode and fuzzy sliding mode controller are also introduced in this chapter.

In chapter 2, the induction machine is modeled with synchronously rotating reference frame. The P-I controllers are designed by pole zero cancellation technique for speed and flux control for the vector controlled induction motor drive by dividing the system into two subsystems i.e. one electrical subsystem and another mechanical subsystem.

In chapter 3, the sliding mode controller is designed for both speed and flux control of induction motor drive. The control law is derived and the gains are selected by designing the controller gains. To achieve the sensorless control, the rotor speed is estimated using direct synthesis of state equations.

In chapter 4, the fuzzy sliding mode controller is designed for the vector controlled induction motor drive. The control law is derived and the similarities of the sliding mode and the fuzzy sliding mode controller are discussed. A symmetrical triangular membership function is selected and the fuzzy variables are chosen such that we get a simple fuzzy rule for the ease of calculation.

Chapter 5 represents the conclusion of the thesis. The simulation responses for different controllers are compared. The assessment of the work and the future scope for the thesis are discussed. The performance comparisons of the controller for a step change in reference rotor speed, step change in load torque and simulation responses for flux weakening mode are made.

1.7 Contribution of the Thesis

The linearized induction motor is simulated for direct vector control. The P-I controller gains are obtained by the pole-zero cancellation technique. Motor speed is estimated by direct synthesis method to develop a sensorless drive, for known advantages. During the parameter variation, the drive's performance degrades, and the motor goes to unstable mode. So, to achieve robustness of the sensorless drive, sliding mode and fuzzy sliding mode controller are designed and compared.

CHAPTER – 2
INDUCTION MACHINE MODELING AND DESIGN OF P-I
CONTROLLERS

2. INDUCTION MACHINE MODELING AND DESIGN OF P-I CONTROLLERS

2.1 Introduction

For the control of any power electronic drive such as an induction motor drive, controllers are designed to control the system. This requires mathematical modeling of the drive, the reason being the higher order nonlinearity and multivariable nature of the systems. By proper mathematical modeling of the plant, the design and development of the power electronics drive systems can be done. The induction motor modeling is mostly done by a three phase (a-b-c) to synchronously rotating (d-q) transformation neglecting saturation, with stator current and rotor flux linkages as the state variables.

In this chapter, modeling of the induction motor and design of the P-I controllers have been presented and the simulated results have been discussed. The nonlinear dynamics of the induction motor are represented by a set of differential equations in a synchronously rotating d-q reference frame with the stator voltages and load torque as the input variables and the electromagnetic torque developed and the rotor angular velocity as the output variables. To design the P-I controllers, the electrical and mechanical subsystems of the induction motor model is represented. These two subsystems are decoupled from each other. The pole placement technique is adopted for the P-I controller design.

2.2 Induction Motor Modeling

The voltage equations of the three phase induction motor in synchronously rotating reference frame are:-

$$V_{ds} = R_s i_{ds} + \frac{d\psi_{ds}}{dt} - \omega_e \psi_{qs} \quad (2.1a)$$

$$V_{qs} = R_s i_{qs} + \frac{d\psi_{qs}}{dt} + \omega_e \psi_{ds} \quad (2.1b)$$

$$V_{dr} = R_r i_{dr} + \frac{d\psi_{dr}}{dt} - (\omega_e - \omega_r) \psi_{qr} \quad (2.1c)$$

$$V_{qr} = R_r i_{qr} + \frac{d\psi_{qr}}{dt} + (\omega_e - \omega_r) \psi_{dr} \quad (2.1d)$$

The electromagnetic torque developed T_e is given by;

$$T_e = \frac{3P}{4} (\psi_{dr} i_{qs} - \psi_{qr} i_{ds}) \quad (2.1e)$$

The torque balancing equation is given by;

$$T_e = T_L + \beta \omega_m + J \frac{d\omega_m}{dt} \quad (2.1f)$$

Where V_{ds}, V_{qs} = Stator d- and q-axis voltages, V_{dr}, V_{qr} = Rotor d- and q-axis voltages in the synchronously rotating reference frame.

ω_m = Rotor mechanical speed in rad/s

ω_r = Rotor electrical speed in rad/s

ω_e = Synchronous electrical speed in rad/s

R_s, R_r = Stator and rotor per phase resistances respectively in ohms (Ω)

ψ_{dr}, ψ_{qr} = Rotor d- and q-axis flux linkage in V.s

ψ_{ds}, ψ_{qs} = Stator d- and q-axis flux linkage in V.s

P = No. of poles

J = Moment of inertia in kg.m^2

β = Coefficient of viscous friction in N.m.s./rad

T_e = Torque developed in N.m.

T_L = Load torque in N.m.

The stator and rotor voltage equations and the electromagnetic torque equations can be represented in matrix form as given below;

$$\begin{bmatrix} V_{ds} \\ V_{qs} \end{bmatrix} = \begin{bmatrix} R_s & 0 \\ 0 & R_s \end{bmatrix} \begin{bmatrix} i_{ds} \\ i_{qs} \end{bmatrix} + \frac{d}{dt} \begin{bmatrix} \psi_{ds} \\ \psi_{qs} \end{bmatrix} + \begin{bmatrix} 0 & -\omega_e \\ \omega_e & 0 \end{bmatrix} \begin{bmatrix} \psi_{qs} \\ \psi_{ds} \end{bmatrix} \quad (2.2)$$

$$\begin{bmatrix} V_{dr} \\ V_{qr} \end{bmatrix} = \begin{bmatrix} R_r & 0 \\ 0 & R_r \end{bmatrix} \begin{bmatrix} i_{dr} \\ i_{qr} \end{bmatrix} + \frac{d}{dt} \begin{bmatrix} \psi_{dr} \\ \psi_{qr} \end{bmatrix} + \begin{bmatrix} 0 & -(\omega_e - p\omega_m) \\ (\omega_e - p\omega_m) & 0 \end{bmatrix} \begin{bmatrix} \psi_{dr} \\ \psi_{qr} \end{bmatrix} \quad (2.3)$$

$$T_e = \frac{3P}{4} \begin{bmatrix} \psi_{dr} & \psi_{qr} \end{bmatrix} \begin{bmatrix} i_{qs} \\ -i_{ds} \end{bmatrix} \quad (2.4)$$

As the rotor windings of the induction motor are short-circuited, so, $V_{dr} = V_{qr} = 0$.

Let, L_s, L_r = stator and rotor self inductances, respectively

L_m = Mutual inductance between stator and rotor

So, neglecting the magnetic saturation of the circuit and iron losses, the flux linkage equations of the circuit can be represented in matrix form as given below:-

$$\begin{bmatrix} \psi_{ds} \\ \psi_{qs} \end{bmatrix} = \begin{bmatrix} L_s & 0 \\ 0 & L_s \end{bmatrix} \begin{bmatrix} i_{ds} \\ i_{qs} \end{bmatrix} + \begin{bmatrix} L_m & 0 \\ 0 & L_m \end{bmatrix} \begin{bmatrix} i_{dr} \\ i_{qr} \end{bmatrix} \quad (2.5a)$$

$$\begin{bmatrix} \psi_{dr} \\ \psi_{qr} \end{bmatrix} = \begin{bmatrix} L_r & 0 \\ 0 & L_r \end{bmatrix} \begin{bmatrix} i_{dr} \\ i_{qr} \end{bmatrix} + \begin{bmatrix} L_m & 0 \\ 0 & L_m \end{bmatrix} \begin{bmatrix} i_{ds} \\ i_{qs} \end{bmatrix} \quad (2.5b)$$

Solving the equation (2.5b) for the rotor currents i_{dr} and i_{qr} , and putting these values in equation (2.5a), we get;

$$\begin{bmatrix} \psi_{ds} \\ \psi_{qs} \end{bmatrix} = \begin{bmatrix} \sigma L_s & 0 \\ 0 & \sigma L_s \end{bmatrix} \begin{bmatrix} i_{ds} \\ i_{qs} \end{bmatrix} + \begin{bmatrix} \frac{L_m}{L_r} & 0 \\ 0 & \frac{L_m}{L_r} \end{bmatrix} \begin{bmatrix} \psi_{dr} \\ \psi_{qr} \end{bmatrix} \quad (2.6)$$

Where $\sigma = 1 - \frac{L_m^2}{L_s L_r} = \text{Leakage Co-efficient}$

Putting the values of rotor d- and q-axis voltage as zero and the values of rotor d- and q-axis currents from equation (2.5b) in (2.3), we get;

$$p \begin{bmatrix} \psi_{dr} \\ \psi_{qr} \end{bmatrix} = \frac{R_r L_m}{L_r} \begin{bmatrix} 1 & 0 \\ 0 & 1 \end{bmatrix} \begin{bmatrix} i_{ds} \\ i_{qs} \end{bmatrix} + \left(-\frac{R_r}{L_r} \right) \begin{bmatrix} 1 & 0 \\ 0 & 1 \end{bmatrix} \begin{bmatrix} \psi_{dr} \\ \psi_{qr} \end{bmatrix} + (\omega_e - p\omega_m) \begin{bmatrix} 0 & 1 \\ -1 & 0 \end{bmatrix} \begin{bmatrix} \psi_{dr} \\ \psi_{qr} \end{bmatrix}$$

or

$$\frac{d}{dt} \begin{bmatrix} \psi_{dr} \\ \psi_{qr} \end{bmatrix} = \begin{bmatrix} a_5 & 0 \\ 0 & a_5 \end{bmatrix} \begin{bmatrix} i_{ds} \\ i_{qs} \end{bmatrix} + \begin{bmatrix} -a_4 & \omega_{sl} \\ -\omega_{sl} & -a_4 \end{bmatrix} \begin{bmatrix} \psi_{dr} \\ \psi_{qr} \end{bmatrix} \quad (2.7)$$

Again, substituting, the values of stator fluxes from equation (2.6) in (2.2), we get,

$$\frac{d}{dt} \begin{bmatrix} i_{ds} \\ i_{qs} \end{bmatrix} = \begin{bmatrix} -a_1 & \omega_e \\ \omega_e & -a_1 \end{bmatrix} \begin{bmatrix} i_{ds} \\ i_{qs} \end{bmatrix} + \begin{bmatrix} a_2 & pa_3\omega_m \\ -pa_3\omega_m & a_2 \end{bmatrix} \begin{bmatrix} \psi_{dr} \\ \psi_{qr} \end{bmatrix} + \begin{bmatrix} \frac{1}{\sigma L_s} & 0 \\ 0 & \frac{1}{\sigma L_s} \end{bmatrix} \begin{bmatrix} V_{ds} \\ V_{qs} \end{bmatrix} \quad (2.8)$$

So, the mathematical model or the state space model of the induction motor in terms of stator currents and rotor flux linkages as the state variables are obtained by combining equation (2.7) and (2.8), as follows.

$$\frac{d}{dt} \begin{bmatrix} i_{ds} \\ i_{qs} \\ \psi_{dr} \\ \psi_{qr} \end{bmatrix} = \begin{bmatrix} -a_1 & \omega_e & a_2 & a_3\omega_r \\ -\omega_e & -a_1 & -a_3\omega_r & a_2 \\ a_5 & 0 & -a_4 & \omega_{sl} \\ 0 & a_5 & -\omega_{sl} & -a_4 \end{bmatrix} \begin{bmatrix} i_{ds} \\ i_{qs} \\ \psi_{dr} \\ \psi_{qr} \end{bmatrix} + \begin{bmatrix} \frac{1}{\sigma L_s} & 0 \\ 0 & \frac{1}{\sigma L_s} \\ 0 & 0 \\ 0 & 0 \end{bmatrix} \begin{bmatrix} V_{ds} \\ V_{qs} \end{bmatrix} \quad (2.9)$$

Where,

$$\begin{aligned}
a_1 &= \frac{1}{\sigma L_s} \left(R_s + R_r \frac{L_m^2}{L_r^2} \right) \\
a_2 &= \frac{1}{\sigma L_s} \frac{R_r L_m}{L_r^2} \\
a_3 &= \frac{1}{\sigma L_s} \frac{L_m}{L_r} \\
a_4 &= \frac{R_r}{L_r} \\
a_5 &= \frac{R_r L_m}{L_r} \\
\omega_{sl} &= \omega_e - \omega_r
\end{aligned} \tag{2.10}$$

The electromagnetic torque developed in terms of state-space variables is:

$$T_e = \frac{3P}{4} \frac{L_m}{L_r} (\psi_{dr} i_{qs} - \psi_{qr} i_{ds}) \tag{2.11}$$

2.3 Design of P-I controllers

The P-I controllers are widely used in industries for high performance electric drives. The gains of the P-I controllers can be designed by well established methods. Also, the P-I controllers are simple to operate and give zero steady state error. But, improper selection of gains may affect the system performance making the system unstable. So, proper selection of gains is quite important. Different techniques can be employed for the design of gains of the P-I controllers. The method used here is pole-zero cancellation technique. The higher order induction motor drive system is divided into two decoupled subsystems i.e., electrical and mechanical subsystem. The P-I controllers are designed for flux and speed control. The two subsystems are shown in fig. 2.1 and fig.2.2.

In the pole-zero cancellation technique, the zero of the P-I controller is chosen so as to cancel one of the open loop poles of the system. Here, the ratio of the integral gain to the proportional gain is kept constant and a suitable value of the natural frequency of the second order system is to be chosen.

2.3.1 Electrical Subsystem

From the mathematical model of the induction motor as given in equation (2.9), we get:

$$\frac{d\psi_{dr}}{dt} = a_5 i_{ds} - a_4 \psi_{dr} + \omega_{sl} \psi_{qr} \quad (2.12)$$

$$\text{and } \frac{di_{ds}}{dt} = -a_1 i_{ds} + \omega_e i_{qs} + a_2 \psi_{dr} + a_3 \omega_r \psi_{qr} + \frac{1}{\sigma L_s} V_{ds} \quad (2.13)$$

For perfect decoupling, $\psi_{qr} = 0$.

Also, the presence of the coupled terms makes the system nonlinear. So, to make the system linear we need to replace these nonlinear coupled terms by u_1 . So, the state-space equations of the induction motor drive for the electrical subsystems, from equation (2.12) and (2.13) can be represented as:

$$\frac{d\psi_{dr}}{dt} = a_5 i_{ds} - a_4 \psi_{dr} \quad (2.12a)$$

$$\text{and } \frac{di_{ds}}{dt} = -a_1 i_{ds} + a_2 \psi_{dr} + u_1 \quad (2.13a)$$

$$\text{where } u_1 = \omega_e i_{qs} + \frac{1}{\sigma L_s} V_{ds}$$

Now, converting the above eqⁿ (2.12a) into s-domain form we get,

$$(s + a_4) \psi_{dr}(s) = a_5 i_{ds}(s) \quad \text{or; } i_{ds}(s) = \frac{s + a_4}{a_5} \psi_{dr}(s). \quad (2.14)$$

Putting the above value of i_{ds} in the s-domain form of eqⁿ (2.13a), we get the transfer function of the electrical subsystem as:

$$(s + a_1) \left(\frac{s + a_4}{a_5} - a_2 \right) \psi_{dr}(s) = u_1(s)$$

$$\text{or, } \frac{\psi_{dr}(s)}{u_1(s)} = \frac{a_5}{s^2 + (a_1 + a_4)s + (a_1 a_4 - a_2 a_5)} \quad (2.15a)$$

So, the block diagram of the linear electrical subsystem is;

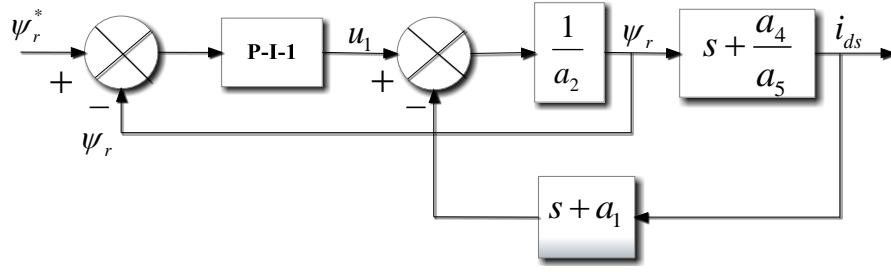


Figure 2.1 Block diagram of electrical subsystem

For perfect decoupling, $\psi_{qr} = 0$, so, $\psi_{dr} = \psi_r$ i.e. the d-axis should coincide with the rotor flux. The induction motor used has the parameter values such as: $a_1 = 302.432$, $a_2 = 245.95$, $a_3 = 23.809$, $a_4 = 10.479$, $a_5 = 5.239$.

Substituting these values in equation (2.15) and factorizing the denominator, we have

$$\text{So, } \frac{\psi_r(s)}{u_1(s)} = \frac{5.239}{(s + 6.1302)(s + 306.7807)}$$

To simplify the design of P-I controller, one pole of the open loop transfer function should be cancelled by the zero of the P-I controller. The transfer function of the P-I controller is;

$$G(s) = K_{p\psi} + \frac{K_{i\psi}}{s} = \frac{K_{p\psi}}{s} \left(s + \frac{K_{i\psi}}{K_{p\psi}} \right)$$

Case-1: To design the P-I controller, let us assume that the pole $(s + 306.7807)$ is to be cancelled

in the open loop transfer function $\frac{i_{ds}}{u_1}$.

$$\text{So, } \frac{K_{i\psi}}{K_{p\psi}} = 306.7807 \text{ or } K_{i\psi} = 306.7807 K_{p\psi}.$$

$$\text{Then, the forward path transfer function is, } G_0(s) = \frac{5.239K_{p\psi}}{s(s + 6.1302)}$$

The closed loop transfer function of the electrical subsystem is given by;

$$\frac{\Psi_r(s)}{\Psi_r^*(s)} = \frac{G_0(s)}{1+G_0(s)} = \frac{5.239K_{p\psi}}{s^2 + 6.1302s + 5.239K_{p\psi}}$$

Let the natural frequency be 50rad/sec. The characteristic polynomial of the closed loop transfer function is of second order and is compared to that of the standard form i.e. $s^2 + 2\xi\omega_n s + \omega_n^2$ and we get the proportional and integral gains such as 477.19 and 146392.7 respectively. For $K_{p\psi} = 477.19$, the roots of the characteristic polynomial obtained are $s = -3.0651 \pm 49.905j$. Due to the imaginary poles, the system is marginally stable.

Case-2: Now, let us assume that the pole at $(s + 6.1302)$ is to be cancelled.

$$\text{So, } \frac{K_{i\psi}}{K_{p\psi}} = 6.1302 \text{ or } K_{i\psi} = 6.1302 K_{p\psi} .$$

$$\text{So, the transfer function of the controller is, } G_0(s) = \frac{5.239K_{p\psi}}{s(s + 306.7807)}$$

So, the closed loop transfer function becomes;

$$\frac{\Psi_r(s)}{\Psi_r^*(s)} = \frac{G_0(s)}{1+G_0(s)} = \frac{5.239K_{p\psi}}{s^2 + 306.7807s + 5.239K_{p\psi}}$$

Now, comparing the characteristic equation of the closed loop transfer function to that of the standard form, we get, $K_{p\psi} = 477.19$ and $K_{i\psi} = 2925.3$.

So, the roots of the characteristic equation, $s^2 + 306.7807s + 477.19 = 0$, has poles at -1.565 and -305.21. The pole at $s = -1.565$ is nearer to the origin of the s-plane as compared to the pole at $s = -6.1302$. So, cancelling the dominant pole is not desirable as it may lead to poor performance reducing the system stability margin.

The pole at $s = -305.21$ is farther from the origin and hence can be cancelled to get a stable system and with good dynamic response.

2.3.2 Mechanical subsystem

The state-space equations of the induction motor drive for the electrical subsystems are:

$$\frac{di_{qs}}{dt} = -\omega_e i_{ds} - a_1 i_{qs} - a_3 \omega_r \psi_{dr} + \frac{1}{\sigma L_s} V_{qs} \quad (2.16)$$

$$\text{and } \frac{d\psi_{qr}}{dt} = 0 = a_5 i_{qs} - \omega_{sl} \psi_{dr} \text{ or } a_5 i_{qs} = \omega_{sl} \psi_{dr} \quad (2.17)$$

The rotor mechanical speed in s-domain form, from the torque balance equation is,

$$\frac{d\omega_m}{dt} = \frac{T_e - T_L - \beta \omega_m}{J} \quad (2.18)$$

When $\psi_{qr} = 0$, from equation (2.11),

$$\text{Electromagnetic torque } T_e = K_t \psi_{dr} i_{qs}, \text{ where } K_t = \frac{3P}{4} \frac{L_m}{L_r}$$

Differentiating the above torque equation and doing appropriate substitution of rate of change of rotor d- axis flux linkage and stator q- axis current and then solving, we get,

$$\frac{dT_e}{dt} = -(a_1 + a_4)T_e + u_2 \quad (2.19)$$

$$\text{Where } u_2 = K_t \psi_{dr} \left[\frac{1}{\sigma L_s} V_{qs} - \omega_r (i_{ds} + a_3 \psi_{dr}) \right] \quad (2.19a)$$

In s-domain form, the open-loop transfer function of the torque is;

$$\frac{T_e(s)}{u_2(s)} = \frac{1}{s + a_1 + a_4} = \frac{1}{s + 312.911} \quad (2.20)$$

The rise time of the torque response of the mechanical subsystem to reach to the steady-state

$$\text{value is 2.3times the time constant i.e. } 2.3\tau_{T_e} = \frac{2.3}{312.911} = 7.34ms.$$

The block diagram of the mechanical subsystem is shown below in Fig. 2.2

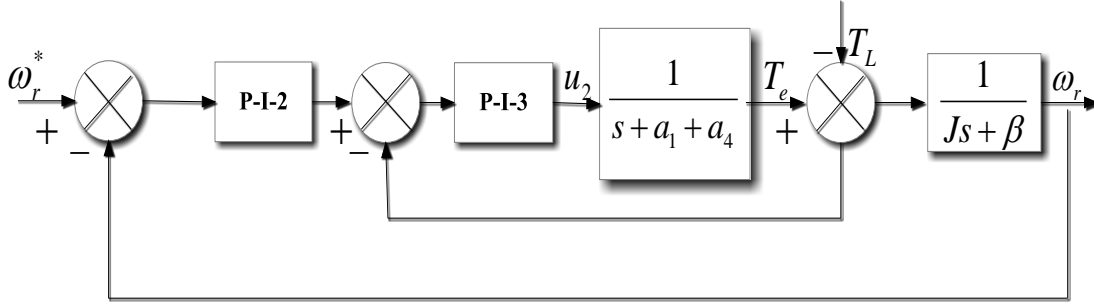


Figure 2.2 Block diagram of mechanical subsystem

The transfer function of P-I torque controller is:
$$G(s) = \frac{K_{pT}}{s} \left(s + \frac{K_{iT}}{K_{pT}} \right) \quad (2.21a)$$

For zero of P-I controller, to cancel the pole of the torque transfer function, the condition will be,

$$K_{iT} = (a_1 + a_4)K_{pT} = 312.911K_{pT}.$$

The closed loop transfer function of the torque loop is,
$$\frac{T_e}{T_e^*} = \frac{K_{pT}}{s + K_{pT}} \quad (2.20b)$$

To make the system such that the feedback torque to follow the command torque, we can choose the value of K_{pT} in order to make the system response instantaneous. So, let $K_{pT} = 100$, then,

$$K_{iT} = 31291.$$

From the above block diagram, the open loop transfer function of speed is:

$$\frac{\omega_r(s)}{u_2(s)} = \frac{1}{(s + a_1 + a_4)(sJ + \beta)} = \frac{1}{(s + 312.911)(s + 0.218)0.16} \quad (2.22a)$$

So, the mechanical time constant of speed is 2.3 times the time constant of speed i.e.

$$2.3\zeta_{or} = \frac{2.3}{0.218} = 10.55 \text{ s.}$$

Now, from the closed loop transfer function of the overall system, we get,

$$\frac{\omega_r(s)}{\omega_r^*(s)} = \frac{K_{p\omega}^* s + K_{i\omega}}{Js^2 + (\beta + K_{p\omega})s + K_{i\omega}} \quad (2.22b)$$

The above equation (2.22b) can also be written as:

$$\frac{\omega_r(s)}{\omega_r^*(s)} = \frac{\frac{K_{p\omega}}{J} * s + \frac{K_{i\omega}}{J}}{s^2 + \frac{(\beta + K_{p\omega})}{J} s + \frac{K_{i\omega}}{J}} \quad (2.22c)$$

Comparing the second order characteristic equation of the closed loop transfer function for speed with the standard second order characteristic equation $s^2 + 2\xi\omega_n s + \omega_n^2$, we can obtain the P-I speed controller gains such as:

$$s^2 + \frac{(\beta + K_{p\omega})}{J} s + \frac{K_{i\omega}}{J} = s^2 + 2\xi\omega_n s + \omega_n^2$$

$$\text{So, } \frac{K_{i\omega}}{J} = \omega_n^2, \text{ or } K_{i\omega} = 0.16 \times 15^2 = 36.$$

$$\text{Also, } \frac{(\beta + K_{p\omega})}{J} = 2\xi\omega_n$$

Considering the system to be critically damped i.e. $\xi = 1$,

$$\text{we get } K_{p\omega} = 2 \times 1 \times 15 \times 0.16 - 0.035 = 4.765$$

Assuming suitable value of the natural frequency as $\omega_n = 15 \text{ rad/s}$. and comparing the

characteristic equation of the closed loop transfer function with that of the standard characteristic equation of the second order system, we can get the gains of the P-I controller for the speed loop.

2.4 Simulation Results and Discussions

In this chapter, the modeling of the induction motor in a synchronously rotating reference frame is done. The vector controlled induction motor drive is modeled in a synchronously rotating d-q reference frame with stator current and rotor flux components as the state variables. P-I controllers are used for the rotor speed and torque control. The P-I controllers are designed by the pole-zero cancellation technique. The system responses are studied and concluded that the speed response is sluggish as compared to that of the torque response and reached to the steady

state slower than the torque response which can be observed by calculating the mechanical time constants of speed and torque respectively from their transfer functions. All this is achieved by making the system decoupled. Thus, the vector controlled induction motor is done with P-I controllers. By deciding the gains of the controller, the simulated results of vector controlled induction motor block diagram are shown below along with the simulated results for different cases.

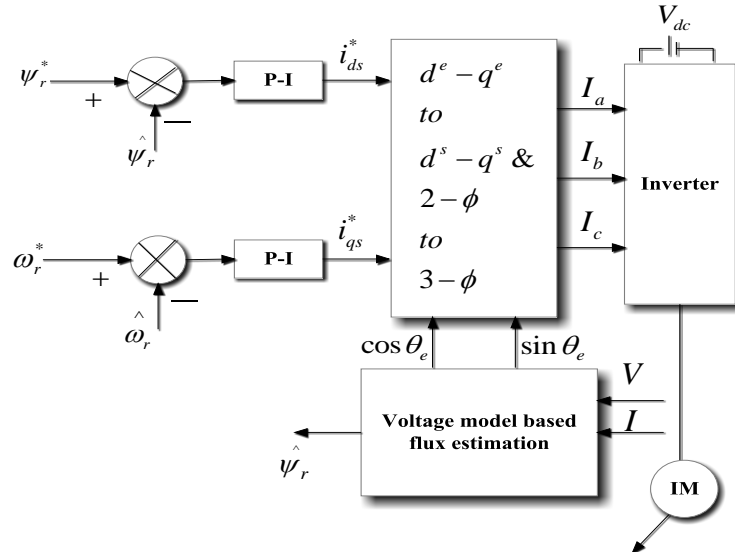


Figure 2.3 Block Diagram for Vector Control of Induction Motor

Case – 1: Step change in reference speed

The rotor reference speed is increased about 20% of the base speed i.e. up to 1734rpm during the time period $t = 2s$ to $t = 4s$. Initially the rotor speed was 1416rpm and with a step change in reference speed, the rotor speed increases to 1696rpm. So, there exists a steady-state speed error which is may be due to the design error in the P-I controller. With this, a rise in the stator phase current occurs from 2.85A to 23A for a transient period and then decreases to 2.85A. An overshoot in the stator d- and q-axis current occurs to a peak value of 20.6A and 21.4A respectively due to the rise in speed and after 0.3s, it comes back to its original steady-state value of 2.36A and 1.88A respectively. This increased rotor speed is maintained from $t = 2s$ to $t = 4sec$ and then it is decreased to its initial speed with the reduction of reference speed from 1734rpm to 1445rpm. So, a negative peak of 17.15A occurs in the stator q-axis current whereas the d-axis stator current reaches to a peak value of 8.652A. A transient disturbance occurs in the

rotor flux for about 0.2s. An electromagnetic torque of 5.1538Nm undergoes a transient disturbance with the variation of rotor speed. The stator q-axis voltage increases to 477V with the rotor speed.

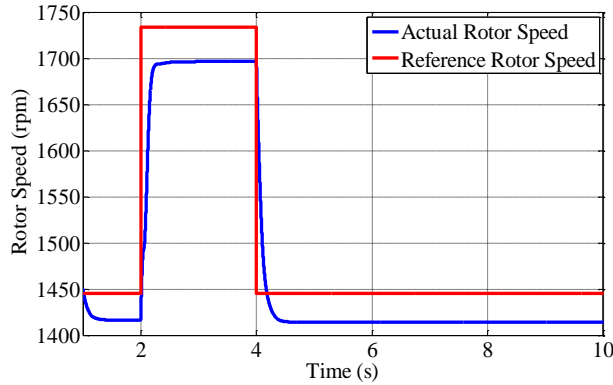


Fig (a)

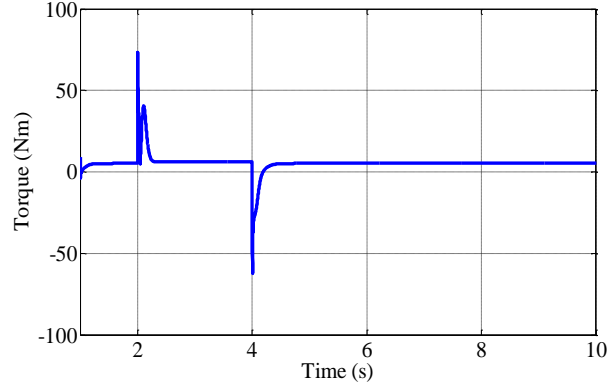


Fig (b)

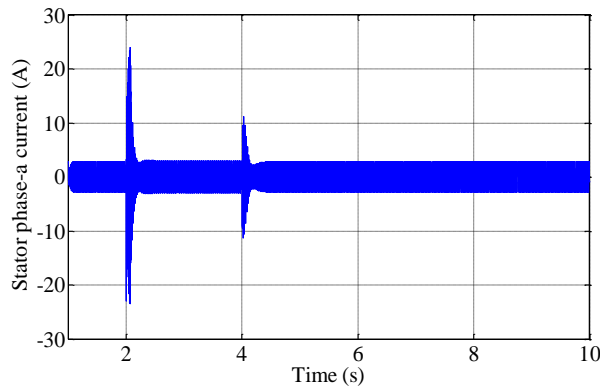


Fig (c)

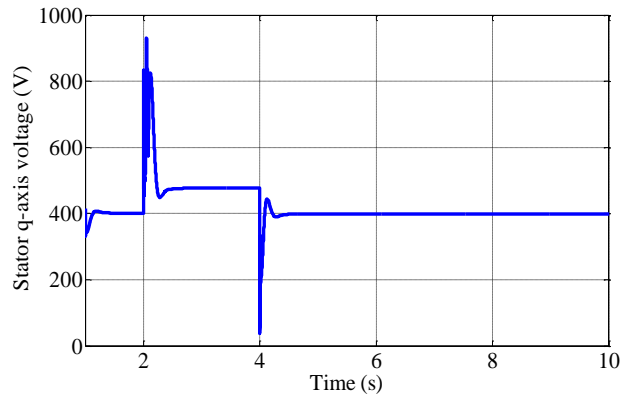


Fig (d)

Figure 2.4 Simulation responses for step change in reference speed

- (a) Rotor reference and actual speed
- (b) Electromagnetic torque
- (c) Stator phase-a current
- (d) Stator q-axis voltage

Case – 2: Trapezoidal change in reference speed

The rotor reference speed is increased linearly from zero to 1734rpm from $t = 0$ to $t = 1$ s, the speed is maintained constant at 1734rpm upto $t = 4$ s and it is observed that the actual rotor speed increases linearly upto 1696rpm within 1sec, though it doesn't match with that of the reference speed. During the trapezoidal change of reference speed, a transient rise of stator d- and q-axis current of about 19A and 19.6A respectively takes place at $t = 1$ s and then it comes to its steady-state value of 2.33A and 1.926A respectively. With the reversal of rotor reference

speed, the stator q-axis current reduces in a ramp manner. At $t = 1$ s, after a transient disturbance, the stator phase-a current settles down at a steady value of 3.02A.

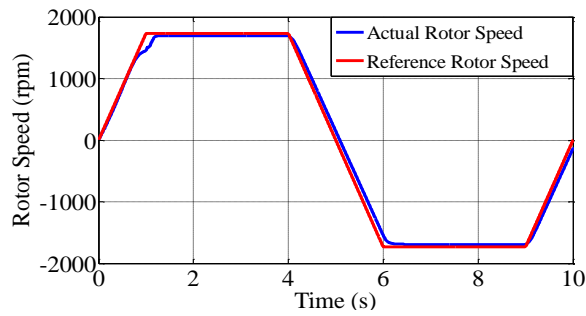


Fig (a)

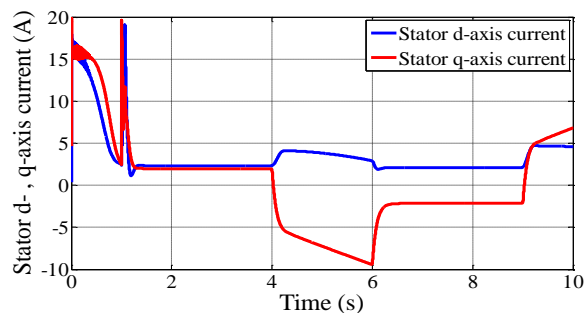


Fig (b)

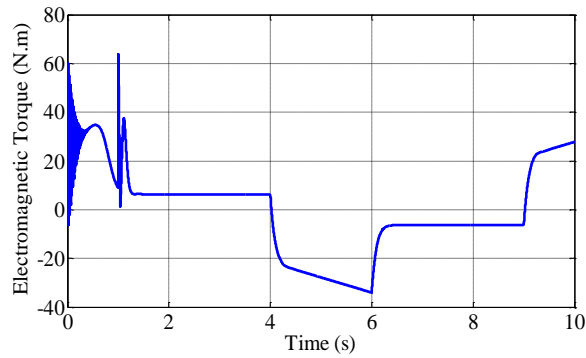


Fig (c)

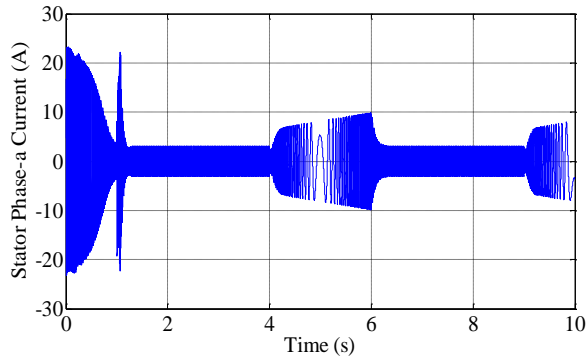


Fig (d)

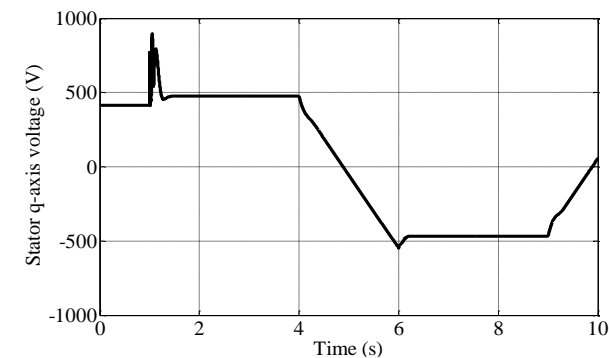


Fig (e)

Figure 2.5 Simulation responses for Trapezoidal change in reference rotor speed

- (a) Rotor reference and actual speed
- (b) Stator d- and q-axis current
- (c) Electromagnetic torque
- (d) Stator phase-a current
- (e) Stator q-axis input voltage

At no-load, the electromagnetic torque of 6.214N.m is produced from $t = 1$ s to $t = 4$ s. With the ramp decrease of rotor speed, the electromagnetic torque decreases in a ramp manner

from $t = 4\text{s}$ to $t = 6\text{s}$. In the reverse motoring mode, the electromagnetic torque of 6.214N.m is produced after $t = 6\text{s}$ to $t = 10\text{s}$. A stator q-axis voltage of 477V is produced and varies according to the variation of rotor speed.

Case – 3: Flux weakening mode:

Fig 2.6 below shows the responses of a vector controlled induction motor drive with a P-I controller with the increase of rotor speed with flux weakening mode. With a variation of rotor reference speed from its base value of 1445rpm to 1734rpm , the actual rotor speed also increases to 1696rpm . During $t = 2\text{s}$ to $t = 4\text{s}$, the region is called as flux weakening region where the flux varies inversely with the rotor speed. The rotor flux takes a settling time of 0.4s to attain its steady value. The stator phase-a current also has a transient overshoot of about 23.5A from 2.9A , and after a transient period of 0.2s , it becomes 2.86A till the rotor speed decreases to its base speed. At $t = 4\text{s}$, with the change of rotor speed to 1445rpm , after a transient disturbance of 0.2s , it goes to its original value of 2.86A . With no load torque applied, the electromagnetic torque developed is 5.38Nm .

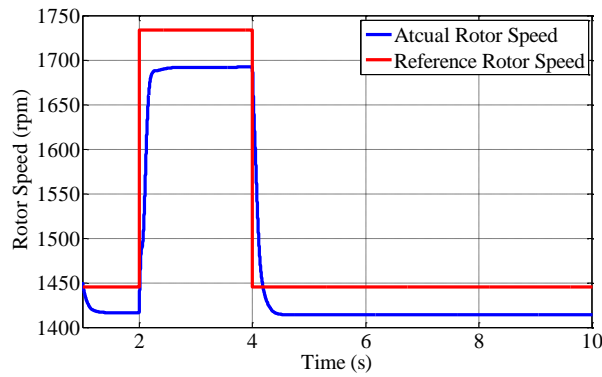


Fig (a)

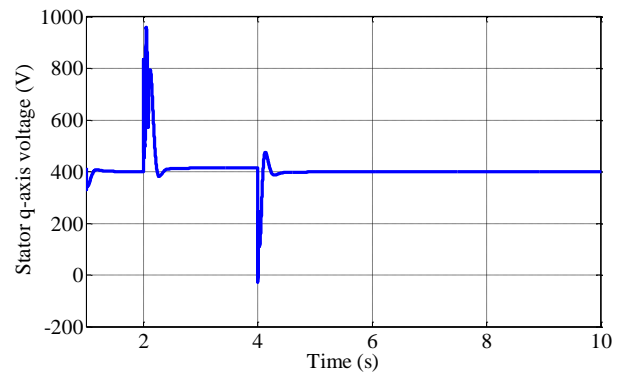


Fig (b)

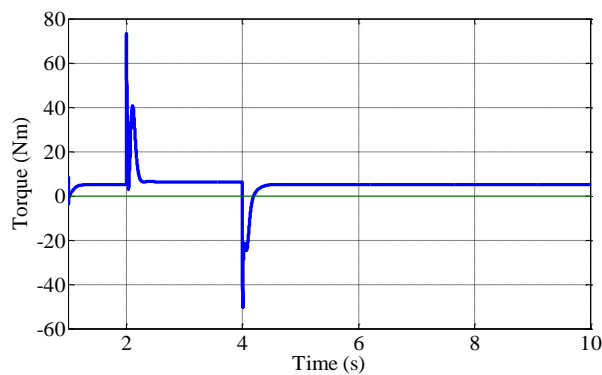


Fig (c)

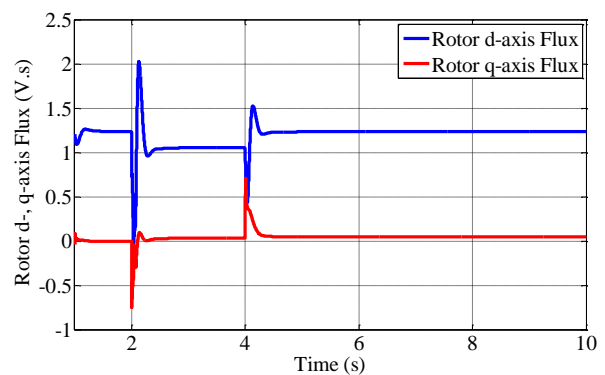


Fig (d)

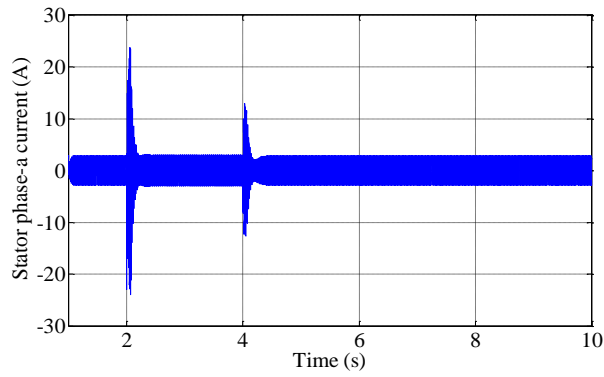


Fig (e)

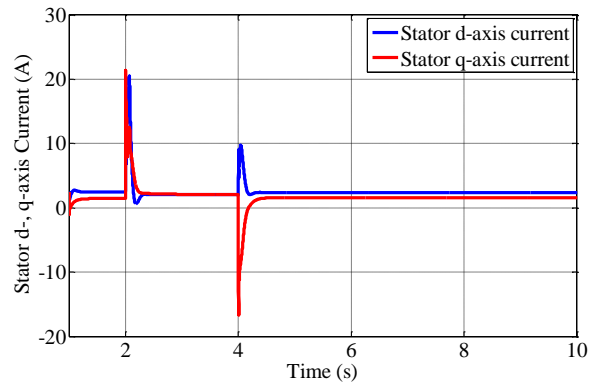


Fig (f)

Figure 2.6 Simulation responses for trapezoidal change in reference speed during flux weakening mode

- (a) Rotor reference and actual speed
- (b) Stator q-axis input voltage
- (c) Electromagnetic torque
- (d) Rotor d- and q-axis flux
- (e) Stator phase-a current
- (f) Stator d- and q-axis current.

Case – 4: Step Change in load torque

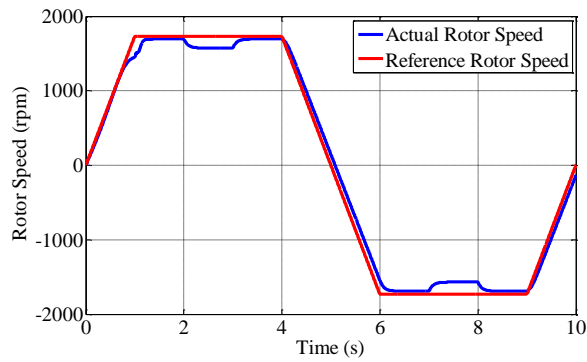


Fig (a)

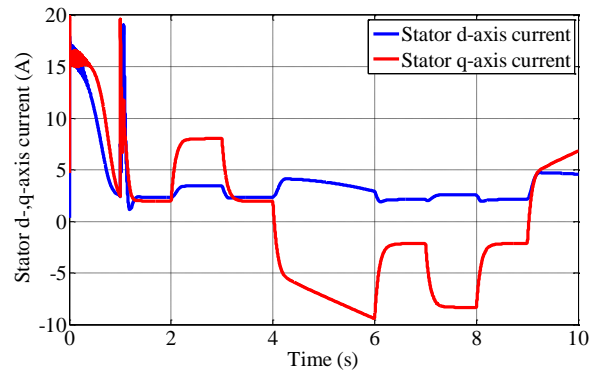


Fig (b)

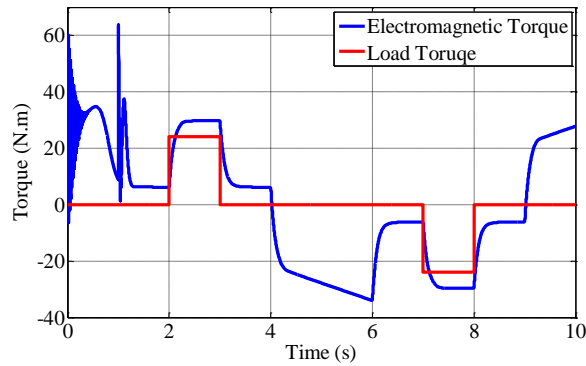


Fig (c)

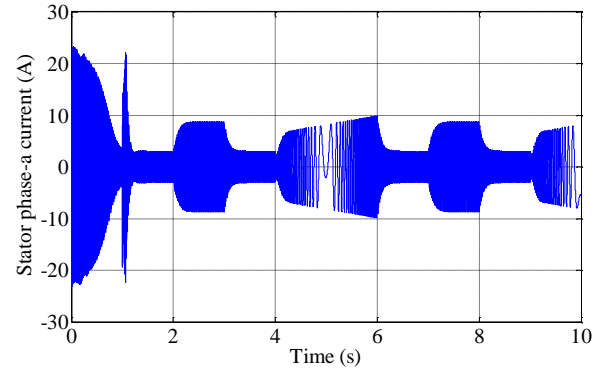


Fig (d)

Figure 2.7 Simulation responses for Step Change in load torque

- (a) Rotor reference and actual speed (b) Stator d- and q-axis current (c) Electromagnetic torque
(d) Stator phase-a current

The simulation responses of vector controlled induction motor with the application of load torque are observed. During $t = 2\text{s}$ to $t = 3\text{s}$, a load torque of 24Nm is applied. The rotor speed falls to 1574rpm due to the application of rated load. With no load, it starts to rotate at its original speed of 1696rpm . The electromagnetic torque develop, after a transient period of 1s , stables at 6.214Nm and during the load applied, it increases to 29.75Nm . When the rated load torque of 24Nm is applied between $t = 7\text{s}$ to $t = 8\text{s}$, during the reverse motoring mode, the developed electromagnetic torque, becoming more negative, reduces to -29.75Nm . The torque component of stator current i.e. stator q-axis current varies accordingly and with the variation of rotor speed. The stator q-axis current rises from 1.926A to 8.013A between $t = 2\text{s}$ and $t = 3\text{s}$ and falls from 2.16A to 8.013A between $t = 7\text{s}$ to $t = 8\text{s}$. The stator q-axis voltage varies with a trapezoidal profile, increases from 477V to 540V with the applied load torque and reduces from 477V to 540V in reverse motoring mode between $t = 7\text{s}$ to $t = 8\text{s}$.

The actual rotor speed, tracks the reference rotor speed, and both the reference and actual rotor speed reduces as a load of $T_L = 24\text{N.m}$ is applied.

2.5 Conclusion

In this chapter, the induction motor is mathematically modeled in a synchronously rotating reference frame and all the simulation studies are done with the synchronously rotating reference frame. The design of P-I controllers is done by dividing the higher order induction motor into two decoupled subsystems in order to determine the P-I controller gain by pole-zero cancellation technique. The analysis of the two subsystems along with the block diagram is shown. The vector controlled induction motor with P-I controller is simulated with different cases such as step and ramp change in rotor reference speed, with consideration of flux weakening mode and with load torque variation. The robustness of the controller was also checked with machine

parameters variation due to temperature changes such as stator and rotor resistances and it is verified that the system is getting unstable due to parameter variations for which frequent tuning of controller gains is required. So, in the next chapter, we go for a nonlinear controller such as sliding mode controller instead of linear P-I controllers.

CHAPTER – 3
DESIGN OF SLIDING MODE CONTROLLERS

3. DESIGN OF SLIDING MODE CONTROLLERS

3.1 Introduction

The control of the higher order dynamical system has many challenges such as its nonlinearity, imprecise physical parameters, coupling of control variables. Induction motors are widely used for industrial purpose. The industrial applications require the variation of speed and load torque with better dynamic performances and with robustness to all perturbations. So, the system can be made robust using sliding mode controller. For this, a control algorithm is desirable for stabilization and for tracking the trajectories.

The sliding mode controller has good performance against the machine unmodeled dynamics, is insensitive to motor parameter variation, capacity for external disturbance rejection and fast dynamics [35]. The induction motor can be employed for position and speed control of an ac servo system. The vector control of induction motor using sliding mode controller is described in this chapter. Also, the chattering problem related to this control technique is focused here.

3.2 Sliding mode controller

The sliding mode control technique is developed from Variable Structure Control (VSC). In variable structure control technique, a surface is defined and the system that we need to control is forced to that surface till the system slides to the desired equilibrium point. So, the surface is named as sliding surface. This surface can be defined by the error and the rate of change of error as the variables. While the system starts sliding on the surface towards the equilibrium point, the system will never be affected by any cause such as any modeling uncertainties or any external disturbances. The condition of the reaching phase can be satisfied by establishing a control law. This control technique can be applied to an n^{th} order system.

If $S(t)$ is the sliding variable, then all the trajectories must reach, slide and remain on the sliding surface $s = 0$. The behavior of the system on the sliding surface is known as sliding mode. So, to bring the state variables into the sliding surface, two conditions are required to be

satisfied, i.e. $s(x,t) = 0$ and $\dot{s}(x,t) = 0$. Here, the sliding mode technique is applied to vector control of induction motor i.e. a second order system.

The vector control of induction motor with sliding mode control technique is described in this section for speed and flux control. To achieve a perfect decoupling, the condition for a field oriented control of induction motor is;

$$\psi_{qr} = 0 \text{ and } \psi_{dr} = \psi_r = \text{constant}$$

$$\text{Form the state space equation; we get that, } \frac{d\psi_{dr}}{dt} = a_5 i_{ds} - a_4 \psi_{dr} \quad (3.1)$$

$$\text{During steady state, } \frac{d\psi_{dr}}{dt} = 0 = a_5 i_{ds} - a_4 \psi_{dr}$$

$$\text{or } \psi_{dr}^* = \frac{a_5 i_{ds}^*}{a_4} \quad (3.1a)$$

Putting the values of motor constants in the above equation, we get,

$$\psi_{dr}^* = L_m i_{ds}^* \quad (3.1b)$$

The speed dynamics from the torque balance equation is,

$$\dot{\omega}_m = \frac{T_e - T_L - \beta \omega_m}{J} \quad (3.2)$$

$$\text{For decoupling, } \psi_{qr} = 0. \text{ So eq}^n \text{ (2.11) becomes, } T_e = K_T \psi_{dr}^* i_{qs} \quad (3.2a)$$

$$\text{Where } K_T = \frac{3P L_m}{4 L_r}$$

$$\text{So, eq}^n \text{ (3.2) becomes, } \dot{\omega}_m = \frac{1}{J} (K_T \psi_{dr}^* i_{qs} - \beta \omega_m - T_L) \quad (3.2b)$$

Let the load torque be considered as the disturbance to the system.

$$\text{So, } \dot{\omega}_m = \frac{1}{J} (K_T \Psi_{dr}^* i_{qs} - \beta \omega_m) + \text{Noise}$$

$$\Rightarrow \dot{\omega}_m = F_1 + \text{Noise} \quad (3.3)$$

Where

$$F_1 = \frac{-\beta}{J} \omega_m + b i_{qs}$$

$$b = \frac{K_T}{J} \Psi_{dr}^*$$

For speed control in vector control of induction motor drive, the condition to be satisfied is;

$$\dot{\omega}_m \Big|_{\omega_m = \omega_m^*} = 0 \quad \text{and} \quad \ddot{\omega}_m \Big|_{\omega_m = \omega_m^*} = 0$$

$$\text{Now, } \ddot{\omega}_m = -\frac{\beta}{J} \dot{\omega}_m + b \dot{i}_{qs} + \text{Noise} \quad (3.3a)$$

The current dynamics of vector controlled induction motor drive is;

$$\dot{i}_{qs} = -\omega_e i_{ds} - a_1 i_{qs} - a_3 \omega_r \Psi_{dr} + \frac{1}{\sigma L_s} V_{qs} \quad (3.3b)$$

$$\text{As } \omega_{sl} = a_5 \frac{i_{qs}}{\Psi_{dr}} \quad \text{and} \quad \omega_e = \omega_r + \omega_{sl}$$

$$\text{Now eq}^n \text{ (3.3b) becomes, } \frac{di_{qs}}{dt} = -\omega_e i_{ds} - a_1 i_{qs} - a_3 \omega_r \Psi_{dr} + \frac{1}{\sigma L_s} V_{qs}$$

$$\text{or, } \frac{di_{qs}}{dt} = -\left(\omega_r + a_4 \frac{i_{qs}}{i_{ds}} \right) i_{ds} - a_1 i_{qs} - a_3 \omega_r L_m i_{ds} + \frac{1}{\sigma L_s} V_{qs} \quad (3.3c)$$

Simplifying the above equation, we get,

$$\dot{i}_{qs} = -(a_1 + a_4) i_{qs} - \omega_r (1 + a_3 L_m) i_{ds} + \frac{1}{\sigma L_s} V_{qs}$$

$$\text{or, } \dot{i}_{qs} = F_2 + \frac{1}{\sigma L_s} V_{qs} \quad (3.4)$$

$$\text{Where, } F_2 = -(a_1 + a_4)i_{qs} - \omega_r(1 + a_3 L_m)i_{ds} \quad (3.4a)$$

The speed dynamics becomes,

$$\ddot{\omega}_m = -\frac{\beta}{J} \dot{\omega}_m + b \dot{i}_{qs} + \text{Noise} \quad (3.5a)$$

Putting the $\dot{\omega}_m$ value in the above equation, we get,

$$\begin{aligned} \dot{\omega}_m &= -\frac{\beta}{J} (F_1 + \text{Noise}) + b \left(F_2 + \frac{1}{\sigma L_s} V_{qs} \right) + \text{Noise} \\ \Rightarrow \ddot{\omega}_m &= -\frac{\beta}{J} F_1 + b F_2 + \frac{b}{\sigma L_s} V_{qs} + D_1 \end{aligned} \quad (3.5b)$$

$$\text{or, } \ddot{\omega}_m = G_1 + u_1 + D_1 \quad (3.5c)$$

$$D_1 = \text{Total disturbance, } \quad u_1 = \frac{b}{\sigma L_s} V_{qs} = \text{Control input, } \quad G_1 = \frac{-\beta}{J} F_1 + b F_2$$

G_1 = Constant which can be estimated from measured values of currents and speed.

Let \hat{G}_1 = estimated value of G_1

ΔG_1 = Error in the estimation of G_1 due to modeling imperfection

$$\text{So, } G_1 = \hat{G}_1 + \Delta G_1 \quad (3.6)$$

$$\text{If } e_\omega = \text{Error in tracking the rotor speed i.e. } e_\omega = \omega_m - \omega_m^* \quad (3.6a)$$

$$\text{Then, } \dot{e}_\omega = \dot{\omega}_m - \dot{\omega}_m^* \quad (3.6b)$$

The sliding surface $s_1(x, t)$ is defined for the speed control and is given by;

$$s_1(x, t) = \left(\frac{d}{dt} + \lambda_1 \right) e_\omega = \dot{e}_\omega + \lambda_1 e_\omega \quad (3.6c)$$

From the state-space equation of the induction motor modeling, the flux dynamics is,

$$\dot{\Psi}_{dr} = -a_4 \Psi_{dr} + a_5 i_{ds} + \omega_{sl} \Psi_{qr} \quad (3.7a)$$

$$\text{And } \ddot{\Psi}_{dr} = -a_4 \dot{\Psi}_{dr} + a_5 \dot{i}_{ds} + \omega_{sl} \dot{\Psi}_{qr} \quad (3.7b)$$

AS $\Psi_{qr} = 0$, so equation (3.7a) becomes $\dot{\Psi}_{dr} = -a_4 \Psi_{dr} + a_5 i_{ds}$

$$\text{or, } \dot{\Psi}_{dr} = F_3 = -a_4 \Psi_{dr} + a_5 i_{ds} \quad (3.7c)$$

$$\dot{i}_{ds} = F_4 + \frac{1}{\sigma L_s} V_{ds} = -a_1 i_{ds} + \omega_e i_{qs} + a_2 \Psi_{dr} + \frac{1}{\sigma L_s} V_{ds} \quad (3.7d)$$

$$\text{Now, } \ddot{\Psi}_{dr} = -a_4 F_3 + a_5 F_4 + \frac{a_5}{\sigma L_s} V_{ds} + \text{Noise}$$

$$\text{or, } \ddot{\Psi}_{dr} = G_2 + u_2 + D_2 \quad (3.7e)$$

$$\text{Where } G_2 = -a_4 F_3 + a_5 F_4 \text{ and } u_2 = \frac{a_5}{\sigma L_s} V_{ds} \quad (3.7f)$$

G_2 = Constant which can be estimated from measured values of currents and flux.

Let \hat{G}_2 = estimated value of G_2

ΔG_2 = Error in the estimation of G_2 due to modeling imperfection

$$\text{So, } G_2 = \hat{G}_2 + \Delta G_2 \quad (3.7g)$$

$$\text{If } e_\psi = \text{Error in tracking the rotor flux i.e. } e_\psi = \Psi_{dr} - \Psi_{dr}^* \quad (3.7h)$$

Then, $\dot{e}_\psi = \dot{\psi}_{dr} - \dot{\psi}_{dr}^*$ (3.7i)

A set of system state trajectories can be defined by a sliding surface for flux control such as,
 $s_2(x,t) = 0$

In the next section, the derivation of control law for both speed and flux control of IM drive is shown.

3.2.1 Control Law for Speed and Flux Control

The derivation of control law for the speed and flux controller is shown below.

A set of system state trajectories can be defined by a sliding surface such as, $s(x,t) = 0$. According to Slotine method, the sliding surface can be defined for an n^{th} order

system such as, $s(x,t) = \left(\frac{d}{dt} + \lambda \right)^{n-1} e$ (3.8a)

Where $\lambda =$ positive constant,

$n =$ Order of the system,

$e =$ Tracking error vector

The sliding mode control should be chosen so as to satisfy the Lyapunov stability criteria:

$$V = \frac{1}{2} s(x)^2 \tag{3.8b}$$

Or, $\dot{V} = s(x) \dot{s}(x)$ (3.8c)

The sliding condition is; $\frac{1}{2} \frac{d}{dt} (s^2) \leq -\eta |s|$

So, $s \dot{s} \leq -\eta |s|$

or, $\dot{s} \operatorname{sgn}(s) \leq -\eta$ (3.8d)

Where
$$\text{sgn}(s) = \begin{cases} 1; s > 0 \\ -1; s \leq 0 \end{cases} \quad (3.8e)$$

For speed control,
$$\dot{s}_1 = \lambda_1 \dot{e}_\omega + \ddot{e}_\omega = \lambda_1 \dot{e}_\omega + G_1 + u_1 + D_1 - \ddot{\omega}_m^* \quad (3.9)$$

So, from eqⁿ (3.8d) and eqⁿ (3.9), we get,

$$\left(\lambda_1 \dot{e}_\omega + G_1 + u_1 + D_1 - \ddot{\omega}_m^* \right) \text{sgn}(s) \leq -\eta_1 \quad (3.10a)$$

or,
$$\left(\lambda_1 \dot{e}_\omega + G_1 + u_1 + D_1 - \ddot{\omega}_m^* \right) \text{sgn}(s) + u_1 \text{sgn}(s) \leq -\eta_1 \quad (3.10b)$$

The sliding mode speed control can be achieved by choosing the control law such as:

$$u_1 = \left(-\hat{G}_1 - \lambda_1 \dot{e}_\omega \right) - K_1 \text{sgn}(s) \quad (3.10c)$$

similarly, for flux control,
$$\dot{s}_2 = \lambda_2 \dot{e}_\psi + \ddot{e}_\psi = \lambda_2 \dot{e}_\psi + G_2 + u_2 + D_2 - \ddot{\psi}_{dr}^* \quad (3.11a)$$

From the sliding condition given in eqⁿ (3.8d), we get that eqⁿ (3.11a) becomes;

$$\left(\lambda_2 \dot{e}_\psi + G_2 + u_2 + D_2 - \ddot{\psi}_m^* \right) \text{sgn}(s) \leq -\eta_2 \quad (3.11b)$$

or,
$$\left(\lambda_2 \dot{e}_\psi + G_2 + u_2 + D_2 - \ddot{\psi}_m^* \right) \text{sgn}(s) + u_2 \text{sgn}(s) \leq -\eta_2 \quad (3.11c)$$

So, the flux control can be achieved by the control law and the control law is given by;

$$u_2 = \left(-\hat{G}_2 - \lambda_2 \dot{e}_\psi \right) - K_2 \text{sgn}(s) \quad (3.11d)$$

From the Lyapunov stability, the positive constants, K_1 and K_2 , also known as the speed and flux controller gain respectively, can be calculated.

The term $K_1 \text{sgn}(s)$ and $K_2 \text{sgn}(s)$ are the controller terms or the correction factors used to satisfy the stability of the speed and flux controller respectively.

The term $\left(-\hat{G}_1 - \lambda_1 \dot{e}_\omega\right)$ and $\left(-\hat{G}_2 - \lambda_2 \dot{e}_\psi\right)$ are the equivalent or compensation terms for the speed and flux controller respectively, that are used to get knowledge of the system dynamics.

3.2.2 Design of the controller's gains

For the speed controller, from eqⁿ (3.10b), we have:

$$\left(\lambda_1 \dot{e}_\omega + G_1 + u_1 + D_1 - \ddot{\omega}_m^*\right) \text{sgn}(s) + u_1 \text{sgn}(s) \leq -\eta_1$$

From eqⁿ (3.10c), substituting the value of u_1 in the above eqⁿ and solving it

we get;

$$K_1 \geq \left(G_1 - \hat{G}_1 + D_1 - \ddot{\omega}_m^*\right)$$

or,

$$K_1 = \left(|\Delta G_{1\max}| + D_{1\max} + \eta_1 + \nu_1\right) \quad (3.12a)$$

Similarly, for flux controller, from eqⁿ (3.10b), we have:

$$\left(\lambda_2 \dot{e}_\psi + G_2 + u_2 + D_2 - \ddot{\psi}_m^*\right) \text{sgn}(s) + u_2 \text{sgn}(s) \leq -\eta_2$$

From eqⁿ (3.11d), substituting the value of u_2 in the above eqⁿ and solving it

We get;

$$K_2 = \left(|\Delta G_{2\max}| + D_{2\max} + \eta_2\right) \quad (3.12b)$$

The controller gains K_1 and K_2 are positive constants that can be determined from eqⁿ (3.12) and stability. The transient response of the system can be improved by increasing the value of the controller gains. If the system has large modeling imperfection and high parameter variations, the error of the controlled variable becomes large. So, with increase in the value of K_1 and K_2 the error of the controlled variable decreases to zero and the state trajectories slide and remain on the

sliding surface $s = 0$. Thus sliding mode can be achieved. But, higher value of controller gains result in chattering. So, proper selection of gains is necessary.

Selection of controller gains

A 5HP induction motor, whose specification and parameters are given in Appendix A1, is selected for deriving the controller gains. The induction motor rotates at a speed of 1445rpm with the stator d-axis rotor flux linkage as a reference value i.e. $\psi_{dr}^* = 1.233\text{V.s}$. The parameters are varied with the rise of temperature. The load torque is varied as a cause of an external disturbance. The rotor reference speed is also varied.

$$\text{The rotor electrical speed } \omega_m = \frac{2\pi N}{60} = \frac{2\pi \times 1445}{60} = 151.32\text{rad/s}.$$

$$\text{The electromagnetic torque developed is } T_e = T_L + \beta\omega_m$$

$$\text{At no load, } T_e = 0.035 \times 151.32 = 5.2962\text{Nm}$$

$$\text{From eq}^n \text{ (3.2a); } i_{qs} = \frac{T_e}{K_T \psi_{dr}^*} = \frac{5.2962}{2.879 \times 1.233} = 1.49\text{A}$$

$$\text{From eq}^n \text{ (3.1b); } i_{ds} = \frac{\psi_{dr}^*}{L_m} = \frac{1.233}{0.5} = 2.46\text{A}$$

$$b = \frac{K_T \psi_{dr}^*}{J} = \frac{2.879 \times 1.233}{0.16} = 22.2\text{rad/s}^2 \cdot \text{A}$$

$$\text{So, } F_1 = -\frac{\beta}{J} \omega_m + b i_{qs} = \frac{-0.035}{0.16} \times 151.32 + 22.2 \times 1.49 = -0.022\text{rad/s}^2$$

$$F_2 = -(a_1 + a_4) i_{qs} - 2\omega_m (1 + a_3 L_m) i_{ds} = -(300.51 + 10.48) 1.49 - 302.64 (1 + 23.3226 \times 0.5) 2.46$$

$$\Rightarrow F_2 = -9889.64\text{A/s}$$

The estimated value of G_1 is:

$$\hat{G}_1 = -\frac{B}{J}F_1 + bF_2 \approx bF_2 = 22.2 \times (-9889.64) = -219.55 \times 10^3 \text{ rad} / \text{s}^3$$

As the two motor constants a_1 and a_4 are dependent on the stator and rotor resistances, so the variation of motor parameters will also vary a_1 and a_4 while a_3 will remain constant.

So, the estimation error due to parameter variation is,

$$\Delta G_1 = -(a_1 + a_4) \times 50\% \times bi_{qs} = -(300.51 + 10.48) \times 50\% \times 1.49 \times 22.2 = -5138.83 \text{ rad} / \text{s}^3$$

$$\text{or, } |\Delta G_1| = 5138.83 \text{ rad} / \text{s}^3$$

Due to modeling imperfection, there may be some estimation error which can be calculated by adding 30% to the above calculated value.

$$\text{So, } |\Delta G_{1max}| = 1.3 \times 5138.83 \approx 6.7 \times 10^3 \text{ rad} / \text{s}^3$$

The load torque is varied from 0 to 24Nm in 2secs. So, the noise introduced into the system is

$$\text{given by; Noise} = \frac{T_L}{J} = \frac{24}{0.16} = 150 \text{ rad} / \text{s}^3.$$

$$\text{So, total noise or disturbance can be calculated as: } D_1 = \frac{150}{2} = 75 \text{ rad} / \text{s}^3$$

The rotor speed is increased by 20% i.e. from 1445r/min to 1734r/min. in 1s. So, the reference value of the acceleration of the rotor speed is:

$$v_1 = 151.32 \times 0.3 = 45.396 \text{ rad} / \text{s}^3$$

$$\text{Let } \eta_1 = 5 \times 10^3 \text{ rad} / \text{s}^2.$$

So, the speed controller gain can be calculated from eqⁿ (3.12a) as,

$$K_1 = (|\Delta G_{1max}| + D_1 + \eta_1 + v_1) = 6.7 \times 10^3 + 75 + 5 \times 10^3 + 45.396 = 11820.4 \text{ rad} / \text{s}^3$$

The gain of the flux controller is calculated as given below. The change or increase in rotor resistance and mutual inductance is also considered here.

The rotor d-axis rotor flux is considered as the reference flux i.e. $\psi_{dr} = \psi_r^* = 1.233V.s$

From eqⁿ (3.7c), $F_3 = -10.48 \times 1.233 + 5.24 \times 2.46 = -0.03144$

From eqⁿ (3.7d), $F_4 = -300.51 \times 2.46 + 314.159 \times 1.49 + 244.405 \times 1.233 = 30.198$

The estimated value of G_2 is: $\hat{G}_2 = -a_4 F_3 + a_5 F_4 = -10.48 \times (-0.03144) + 5.24 \times 30.198 = 158.56$

The estimation error is due to parameter variation such as R_r and L_m . So the motor constants a_1, a_2, a_4 and a_5 will vary. So, the estimation error due to parameter variation is,

$$|\Delta G_2| = \hat{G}_2 \times 50\% = 79.28$$

Let $\eta_2 = 1.6 \times 10^3 \text{ rad} / \text{s}^2$

The noise can be calculated as, $Noise = \omega_{sl} \psi_{qr} = \text{negligible as } \psi_{qr} \approx 0$.

Now, $K_2 = (|\Delta G_{2\max}| + D_{2\max} + \eta_2) = 79.28 + 0 + 1600 = 1679.28$

3.3 Rotor Speed Estimation

The speed estimation is an important aspect for high performance field oriented control of IM drive. Without mechanical speed sensor, the induction machine drive becomes more reliable, less cost and small is size. Many speed estimation algorithms have been developed since last few years.

The simple techniques adopted here for the speed estimation are speed estimation from the state equations of the induction motor. From the dynamic state equations of induction machine, the speed signal is generated directly. The rotor angle can be determined from the rotor d- and q-axis fluxes in synchronously rotating reference frame,

$$\text{i.e. } \angle \theta_e = \tan^{-1} \left(\frac{\Psi_{qr}}{\Psi_{dr}} \right) \quad (3.12c)$$

Differentiating the above eqⁿ (3.12c), we get,

$$\frac{d\theta_e}{dt} = \frac{\Psi_{dr} \times \dot{\Psi}_{qr} - \Psi_{qr} \times \dot{\Psi}_{dr}}{\Psi_r^2} \quad (3.12d)$$

Thus, the estimated speed $\hat{\omega}_r$ can be calculated by eqⁿ (3.12e) as given below.

$$\hat{\omega}_r = \frac{d\theta_e}{dt} - \frac{L_m}{T_r} \left[\frac{\Psi_{dr} \times \dot{i}_{qs} - \Psi_{qr} \times \dot{i}_{ds}}{\Psi_r^2} \right] \quad (3.12e)$$

3.4 Simulation Results and Discussions

The vector controlled induction motor drive is simulated with the sliding mode controller. The simulated results are discussed here with the different cases. The different cases simulated here are:

- (a) Step change in reference speed
- (b) Trapezoidal change in reference speed
- (c) Step change in load torque
- (d) Parameter variation such as stator and rotor resistances

Case-1: Step change in reference speed

The reference speed is increased by 20% of the base speed i.e. from 1445rpm to 1734rpm after $t = 2s$ and is then decreased after $t = 4s$ to the base speed with the load torque kept at zero. The actual rotor speed follows the reference rotor speed. The reference rotor d-axis flux is kept constant at 1.233V.s. The field weakening mode is not considered here. So, irrespective of the change in rotor speed, the rotor flux is kept constant between $t = 2s$ to $t = 4s$ and the q-axis rotor flux remains at zero value. After $t = 1s$, the stator q-axis current becomes constant at 1.491A. With the increase in rotor speed upto 1734rpm at $t = 2s$, a transient disturbance occurs and the current value increases to 14.6A which is less than twice the rated current. As the rotor speed settles at 1734rpm, the torque component of stator current reduces to its steady state value of

1.789A. Similarly, with the decrease of rotor speed to its base value, a transient disturbance occurs and the torque component of stator current comes to its steady value of 1.491A after the transient period. The d-axis stator current remains constant at 2.467A. The stator phase-a current, has a peak value of 2.88A. During the transient disturbance due to the increase and decrease of rotor speed at $t = 2s$ and at $t = 4s$ respectively, the stator phase current undergoes a transient disturbance and then reaches a steady state value of 2.882A. The response of stator q-axis input voltage and the control inputs for both the speed and flux controller are shown. An instantaneous rise of stator q-axis voltage happens with the increase in rotor speed and after a transient disturbance, it comes to its final value. The response for control law input for sliding mode controller is also shown. A transient rise upto 48395rad/s^3 occurs in the control input for speed controller due to the step change in rotor speed whereas the initial rise in the control input is due to the transient period of the system before the steady state i.e. before $t = 2s$.

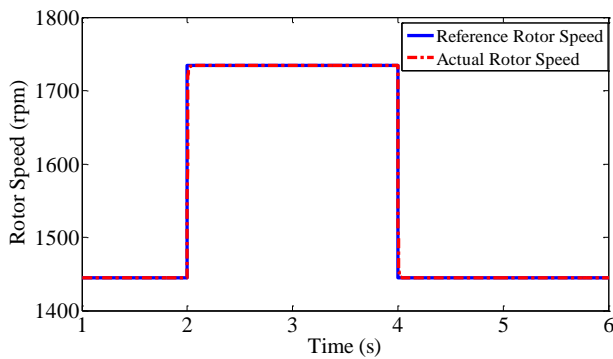


Fig (a)

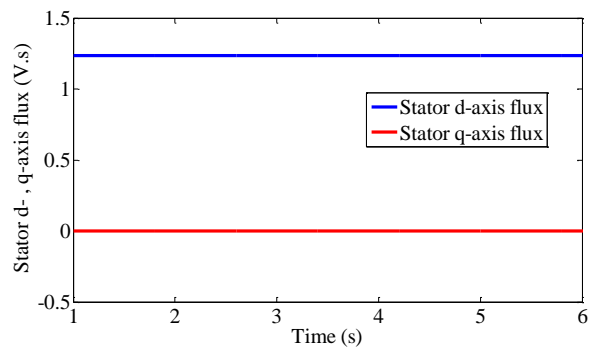


Fig (b)

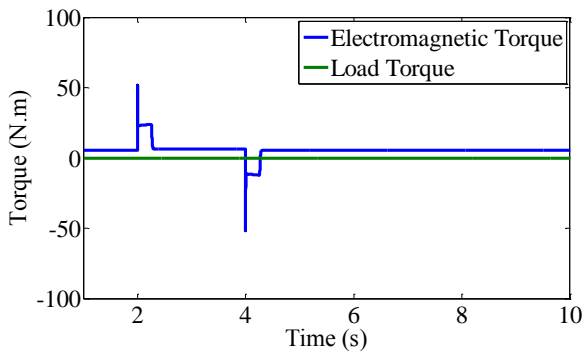


Fig (c)

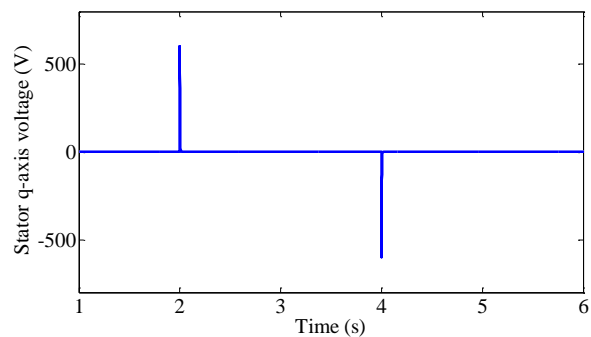


Fig (d)

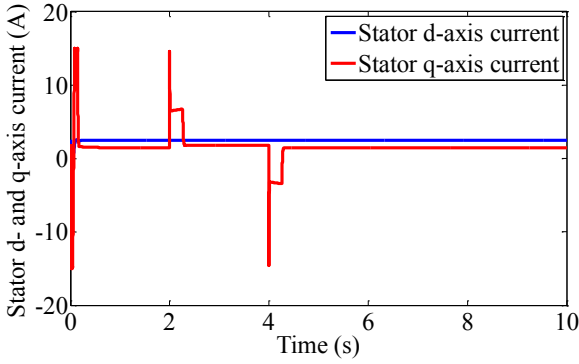


Fig (e)

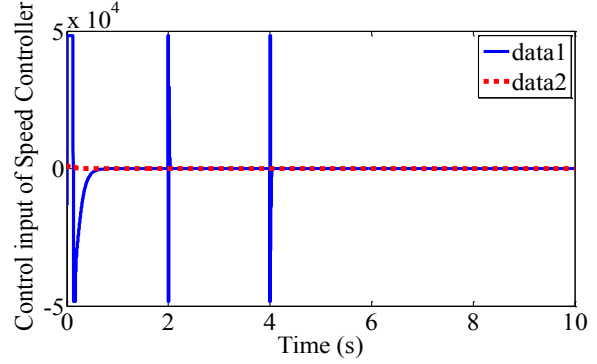


Fig (f)

Figure 3.1 Simulation responses for step change in reference speed

(a) Rotor reference and actual speed (b) Rotor d- and q-axis flux (c) Electromagnetic Torque developed (d) Stator q-axis input voltage (e) Stator d- and q-axis current (f) Control input for speed and flux controller.

Case-2: Variation of rotor speed with a trapezoidal profile

The reference rotor speed is varied in a trapezoidal manner. The rotor speed is increased to 1734rpm in a ramp manner till $t = 1s$ and the rotor continues to rotate at this speed there upto $t = 4s$. The actual rotor speed follows the reference rotor speed since start-up with zero speed error. The stator d-axis current has a steady state value of 2.467A whereas the stator q-axis current varies according to the variation in speed. During the speed reversal, the stator q-axis current decrease and reaches to a negative peak of 9.96A. In the reverse motoring mode, from $t = 6s$ to $t = 9s$, the torque component of stator current has a magnitude of 1.789A flows and at $t = 9s$, with the increase of rotor speed, it starts to increase and reaches to a peak value of 9.96A. The electromagnetic torque varies in proportion with the stator q-axis current. At no load, the electromagnetic torque developed is 5.2962Nm. The induction motor rotating at its base speed develops a maximum torque of 35.408Nm irrespective of the magnitude. As the field weakening mode is not considered, the rotor d-axis flux remains constant at 1.233V.s whereas the rotor q-axis flux remains at its zero value to ensure perfect decoupling. The response of the control input for speed controller is shown. A rise of upto 48395 rad/s^3 occurs in the control input due to the transient disturbance and then settles at zero. A spike exists at $t = 1s$ with the linear increase of rotor speed, and during the speed reversal at $t = 4s$ and the control input increases to a negative peak of 48395 rad/s^3 . Similarly, at $t = 6s$ and at $t = 9s$, the control input goes to a

positive peak of 48395rad/s^3 . The peak value of stator phase-a current during steady state is 3.04A. The q-axis stator voltage varies with the rotor speed and reaches a steady state value of 489.75V. The control law for the sliding mode flux controller response is also shown here. With a starting peak value of 1600rad/s^3 , the control input for the flux controller becomes zero.

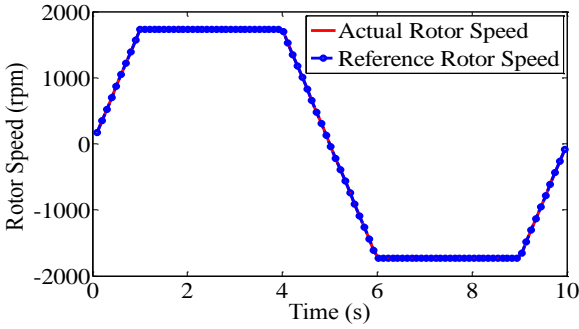


Fig (a)

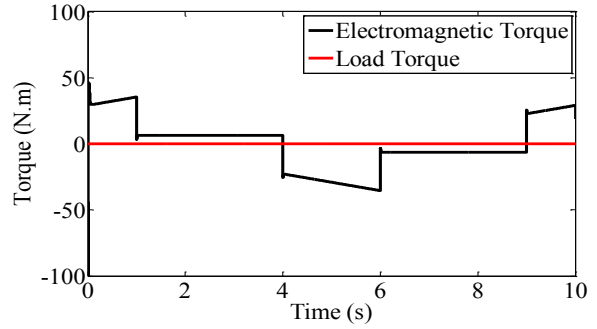


Fig (b)

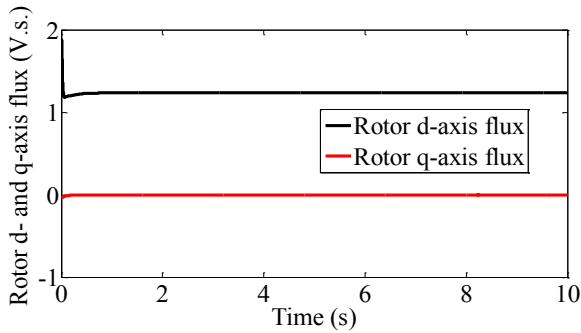


Fig (c)

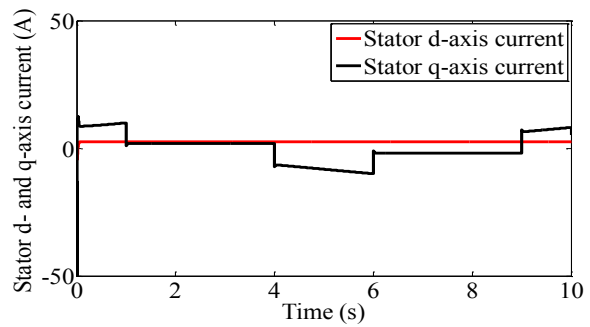


Fig (d)

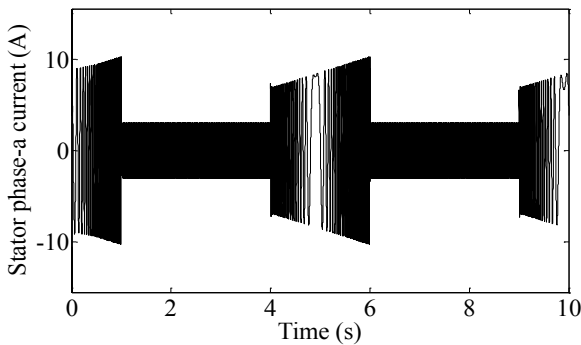


Fig (e)

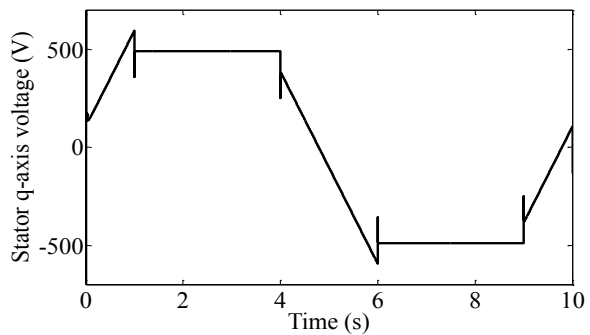


Fig (f)

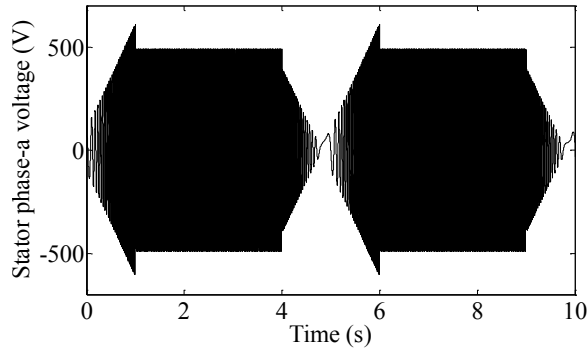


Fig (g)

Figure 3.2 Simulation responses for trapezoidal change in Reference rotor speed

(a) Rotor reference and actual speed (b) Electromagnetic torque (c) Rotor d- and q-axis flux (d) Stator d- and q-axis current (e) Stator Phase-a Current (f) Stator q-axis Control input voltage (g) Stator Phase-a voltage.

Case-3: Field weakening mode

The effect of increasing rotor speed above the base speed on the rotor d-axis flux is observed. With the step change in reference rotor speed from 1445rpm to 1734rpm i.e. 20% above the base speed, the rotor d-axis flux decreases from its constant value of 1.233V.s to 1.028V.s. This is known as flux weakening mode where the rotor flux varies inversely as the rotor speed increases. The q-axis rotor flux remains constant at zero. The rotor rotates at an increased speed of 1734rpm from $t = 2s$ to $t = 4s$ and then decreases to its original value. It is observed that due to the change in rotor flux, the flux component of stator current decreases from 2.467A to 2.056A from $t = 2s$ to $t = 4s$ weakens and then returns to its original value with the decrease of rotor speed to its base speed. The stator q-axis current, being the function of rotor speed, varies with the change in rotor speed. With a step increase of rotor speed, the torque component of stator current increases from 1.491A to 2.147A after a transient disturbance of 0.4s.. During flux weakening mode, the control input for sliding mode flux controller undergoes a transient disturbance for about 0.05s due to the decrease in rotor flux. The instant where the change in rotor flux occurs due to the increased rotor speed from its base value, i.e. in flux weakening mode, the control input for both speed and flux controller undergoes a transient disturbance at that instant. During the transient disturbance, the control input for speed and flux

controller goes to a peak value of magnitude 48400rad/s^3 and 1600rad/s^3 respectively. The rotor d-axis versus q-axis flux plot is shown below.

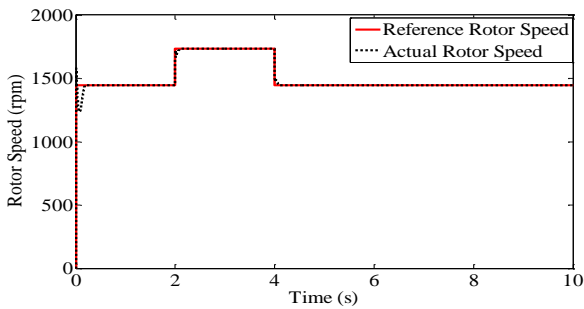


Fig (a)

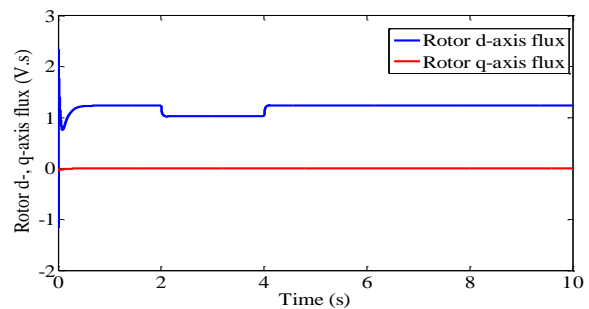


Fig (b)

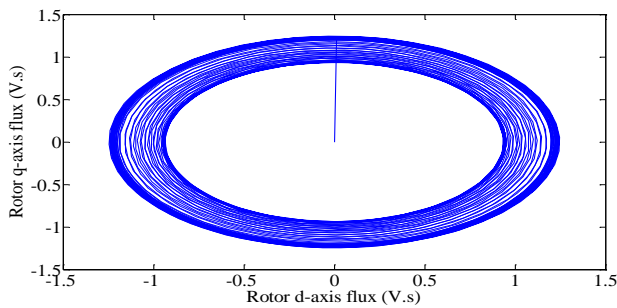


Fig (c)

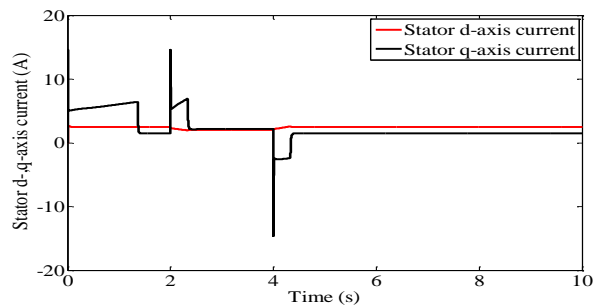


Fig (d)

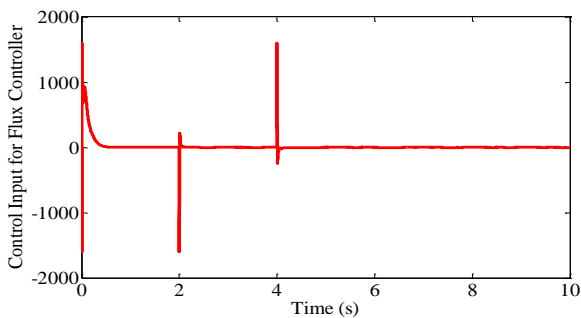


Fig (e)

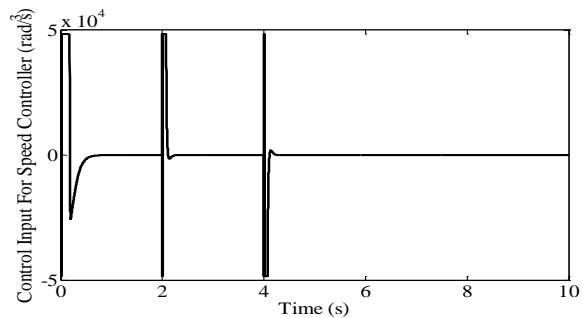


Fig (f)

Figure 3.3 Simulation responses for Step Change in Reference Speed during Flux Weakening Mode

(a) Rotor reference and actual speed (b) Rotor d- and q-axis flux (c) Rotor d-axis flux vs q-axis flux plot (d) Stator d- and q-axis current (e) Control input for flux controller (f) Control input for speed controller

Case-4: Step change in load torque

A rated load torque of magnitude 24N.m is applied between $t = 2\text{s}$ to $t = 3\text{s}$ during the forward motoring mode and between $t = 7\text{s}$ to $t = 8\text{s}$ during the reverse direction of the rotor. With the increase in load torque in forward motoring mode, the electromagnetic torque developed increases and during $t = 6\text{s}$ to 7s , during reverse motoring mode, the electromagnetic torque developed decreases by removing the load torque and the simulated responses are studied. With sliding mode controller, with the application of load torque, the rotor speed decreases from 1734rpm to 1732rpm after a transient disturbance of 0.045s and then comes to its original speed. With the application of full load torque at $t = 2\text{s}$, the stator flux component of current remains constant at 2.467A whereas the stator torque component of current varies with the variation of electromagnetic torque i.e. increases from 1.789A to 8.546A and again decreases to 1.789A as the load becomes zero at $t = 3\text{s}$. The stator q-axis voltage increases from 489.75volts to a peak value of 576.24V between $t = 2\text{s}$ and $t = 3\text{s}$, then it reduces to its original value.

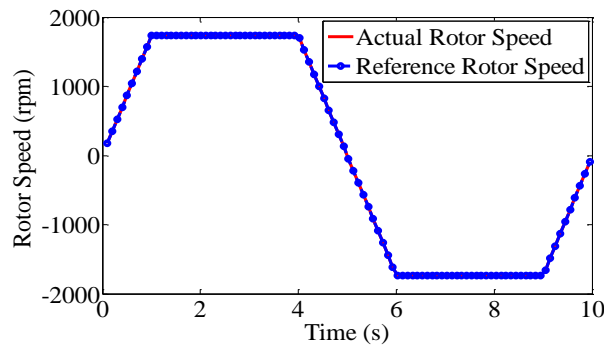


Fig (a)

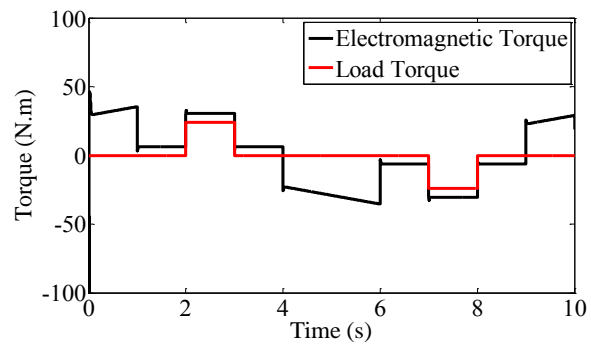


Fig (b)

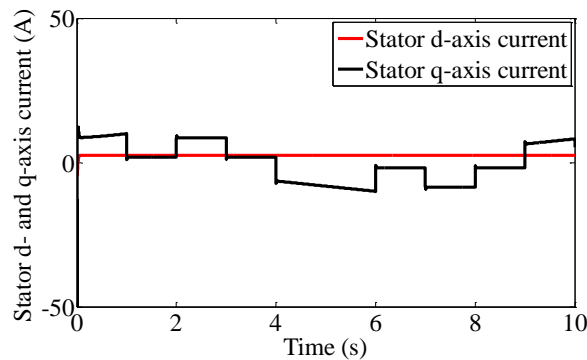


Fig (c)

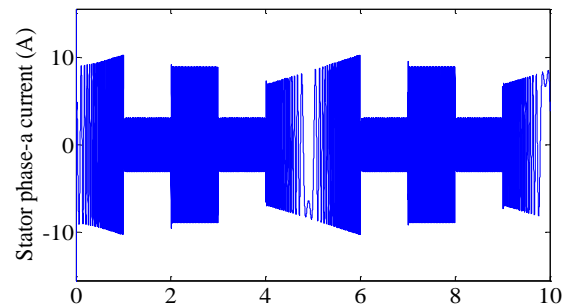


Fig (d)

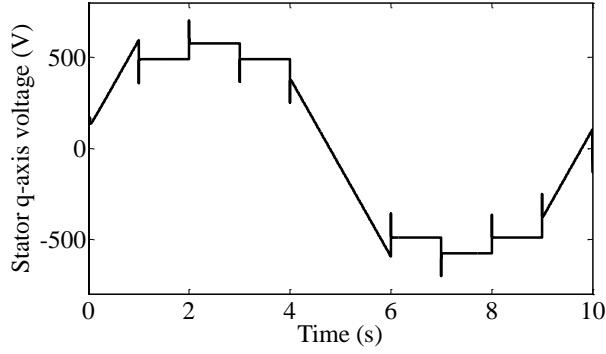


Fig (e)

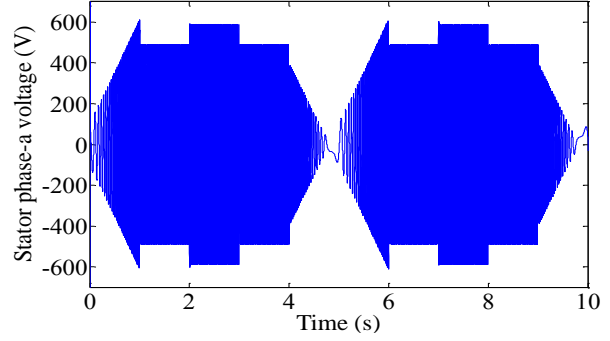


Fig (f)

Figure 3.4 Simulation responses during Change of Load Torque

- (a) Reference and actual rotor speed
- (b) Change of load torque
- (c) Stator d- and q-axis current
- (d) Stator Phase-a Current
- (e) Stator q-axis voltage
- (f) Stator phase-a voltage

Case-5: Parameter variations such as stator and rotor resistances

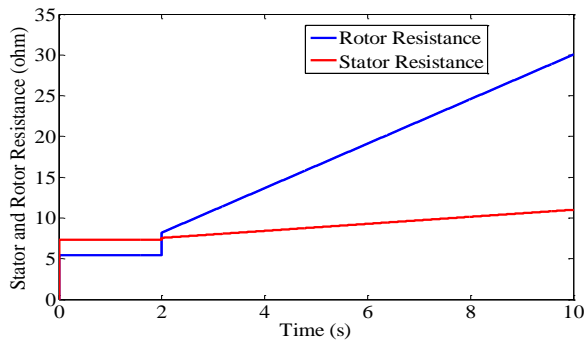


Fig (a)

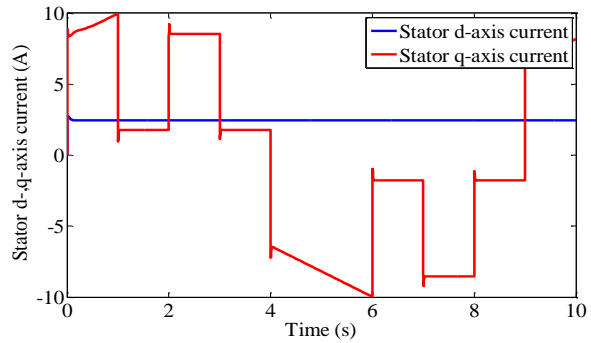


Fig (b)

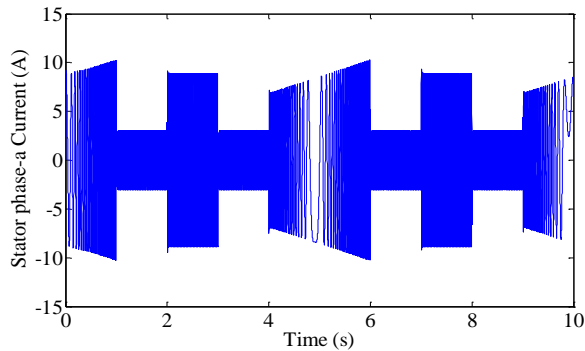


Fig (c)

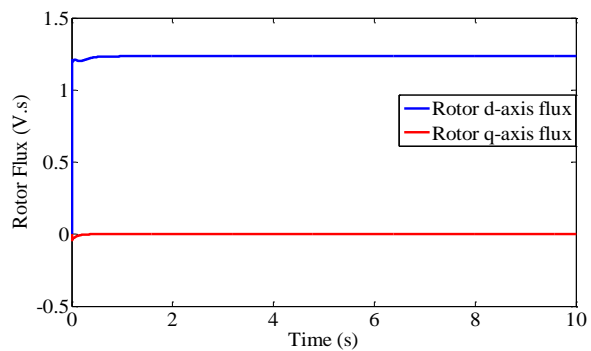


Fig (d)

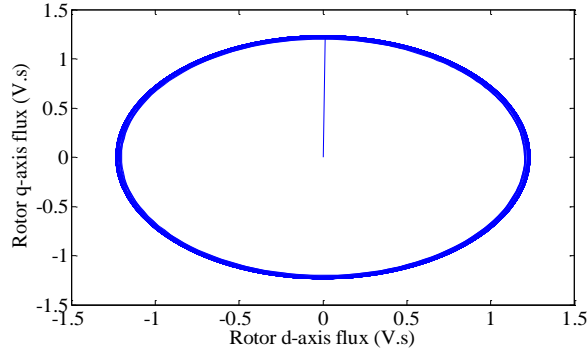


Fig (e)

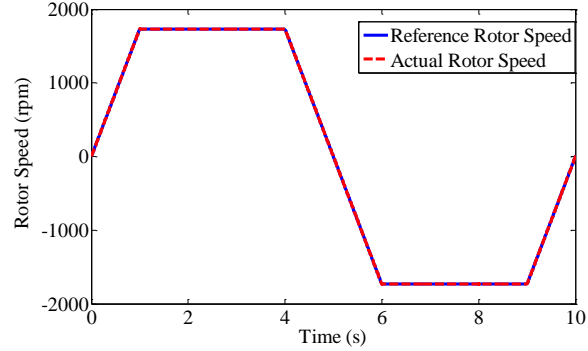


Fig (f)

Figure 3.5 Simulation responses during Change of motor parameter variation

(a) Rotor and stator resistance (b) Stator d- and q-axis current (c) Stator Phase-a Current (d) Rotor d- and q-axis flux (e) Rotor d-axis plot versus q-axis plot (f) Reference and actual rotor speed

With the increase in rotor speed, the temperature increases and the induction motor parameters are varied such as stator and rotor resistances as they vary with the change in temperature and load. The nature of various responses of the stator and rotor dependent parameters is studied under parameter variations and the robustness of the sliding mode controller is verified. At $t = 2s$, during the transient period, the rotor resistance remains constant. After $t = 2s$, with the linear increase in rotor speed and with the passage of time, the rotor resistance increases from 5.46Ω to 30Ω i.e. the rotor resistance becomes 5.5times the actual rotor resistance and the responses of the induction motor are observed. Also, after $t = 2s$, the stator resistance increases from its actual value of 7.34Ω to 11.008Ω i.e. about 1.5times its actual value with the increase in temperature. The responses of different stator currents, stator phase voltage and the rotor flux graphs are observed. The rotor d-axis versus rotor q-axis flux plot is a unit circle with constant rotor d-axis flux and zero q-axis flux. The robustness is verified with the system remaining in stable state irrespective of the parameter variation.

3.5 Conclusion

The induction motor is modeled and the speed and flux controller is designed with sliding mode controller. The control laws are discussed and the procedure to determine the controller gains is derived. The controller gains are selected taking the parameter variations and noise into consideration. The chattering problem can be reduced by introducing the saturation function. The

rotor speed is estimated by the direct synthesis of state equations and the error in speed is observed. The system responses are observed, studied and irrespective of the variation of induction motor parameter variation such as stator and rotor resistance with the temperature, speed and load torque variation and the flux weakening mode are verified that the performance of sliding mode controller is satisfactory.

CHAPTER – 4

DESIGN OF FUZZY SLIDING MODE CONTROLLERS

4. DESIGN OF FUZZY SLIDING MODE CONTROLLERS

4.1 Introduction

Vector controlled Induction motor drive gives robust performance against parameter variations, machine modeling inaccuracies, external disturbances. Irrespective of many advantages of sliding mode controller, it is associated with the chattering problem and needs the accurate knowledge of the system. The inclusion of saturation function to reduce the chattering problem can be eliminated by a hybrid controller known as fuzzy sliding mode controller. This hybrid controller gives a chattering free and robust satisfactory performance without the accurate knowledge of the system dynamics.

Fuzzy logic controller is a simple rule based controller. The principle of sliding mode and fuzzy logic controller are combined together to form the fuzzy sliding mode controller. For higher order nonlinear systems, the inclusion of saturation function and high value of controller gain can be avoided by combining the fuzzy logic controller with the sliding mode controller. In this chapter, the speed of the vector controlled induction motor drive is controlled by this hybrid controller and the performance of the system and the responses are studied.

4.2 Qualitative Aspects of Fuzzy Rule Design

The rules of the sliding mode fuzzy controller with respect to the normalized phase plane are:

- ❖ The normalized fuzzy output should be negative above and positive below the switching line.
- ❖ The fuzzy control output should be increased as the distance between the actual state and the switching line $s = 0$ increases. If D_1 is the distance between the actual state and the switching line $s = 0$, and if D_1 increases, then the fuzzy control output should increase.

The distance D_1 is given by; $D_1 = \frac{|s|}{\sqrt{1+\lambda^2}}$, where $s = \dot{e} + \lambda e$.

- ❖ The fuzzy control output should be increased as the distance between the actual state and the line perpendicular to the switching line $s = 0$ increases. If D_2 is the distance between

the actual state and the switching line $s = 0$, and if D_2 increases, then the fuzzy control output should increase. The distance D_2 is given by; $D_2 = \sqrt{e^2 + \dot{e}^2 - D_1^2}$.

- ❖ The normalized value of the error and the rate of change of error should be by the maximum values of the normalized fuzzy output according to the sign of the normalized fuzzy output.

4.3 Design of Fuzzy Logic Controller

The fuzzy logic controller consists of the following stages:

1. Normalization
2. Fuzzification
3. Inference Mechanism
4. Defuzzification
5. Denormalization

Normalization maps the physical values of the current systems state variables into a normalized universe of discourse. The error and rate of change of error of the control variables are mapped into normalized value of the output variables into physical domain.

Fuzzification is a process of converting crisp variables into fuzzy or linguistic variables. The fuzzy variables chosen for the normalized distances are zero (Z) and positive small (PS) and the fuzzy variables of the normalized controller gain are zero (Z), positive small (PS) and positive big (PB). For the ease of calculation, the membership function chosen here is triangular membership function.

The inference mechanism is an important part of the fuzzy logic controller. Here, the If-Then linguistic rules or statements are used to determine the fuzzy rules by which the human decision making based on fuzzy logic can be simulated. These fuzzy rules are used to determine the controller gain. By using the max-min algorithm, the fuzzy rules can be expressed.

Defuzzification is the process that converts the fuzzy variables into crisp variables. This transformation is done by the membership functions where a nonfuzzy control action is yielded

from an inferred fuzzy control action. The best well known method used for the defuzzification process is centre of area (COA) method. The defuzzified output calculated by this method is;

$$K_{fuzzy,N} = \frac{\int \mu_{out} \cdot K_n \cdot dK_n}{\int \mu_{out} \cdot dK_n}$$

The process of denormalizing the defuzzified normalized crisp output with respect to the corresponding physical domain is known as denormalization. This can be done by choosing a

$$\text{suitable denormalization factor } N = \frac{K_{fuzzy,max}}{K_{fuzzy,N max}}$$

4.4 Design of Fuzzy Sliding Mode Controller

To design a fuzzy sliding mode controller, a sliding mode controller is developed by introducing a fuzzy sliding mode controller.

For a fuzzy sliding mode controller, the block diagram is:

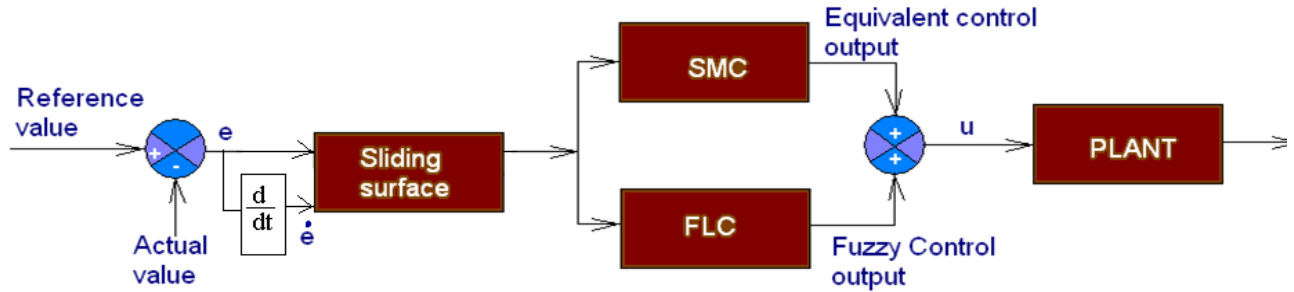


Fig 4.1 Block Diagram of Fuzzy Sliding mode Controller

$$u = \left(-\hat{G} - \lambda \dot{e} \right) - K \operatorname{sgn}(s) \quad (4.1a)$$

Where, $\left(-\hat{G} - \lambda \dot{e} \right) =$ Compensation Term

$K \operatorname{sgn}(s) =$ Controller gain term

For a fuzzy logic controller, the working principle is:

$$u_{fuzzy} = -K_{fuzzy} \operatorname{sgn}(s) \quad (4.1b)$$

So, combining the two principles, we get the working principle of fuzzy sliding mode controller with estimation of system dynamics is:

$$u = \left(-\hat{G} - \lambda \dot{e} \right) + u_{fuzzy}$$

Where u_{fuzzy} = Fuzzy control output

$$u = \left(-\hat{G} - \lambda \dot{e} \right) - K_{fuzzy} \operatorname{sgn}(s) \quad (4.1c)$$

In fuzzy sliding mode controller, a phase plane is derived by an error (e) and the rate of change of error (\dot{e}) of the state variables that are required to be controlled.

The fuzzy logic controller has two inputs and an output, the error and the rate of change of error are treated as the two inputs and the controller gain is treated as an output.

Let the two crisp inputs be e and \dot{e}

Where e = Error of the control variable

\dot{e} = Rate of change of error of the control variable

N_1, N_2 = Normalization Factors

The two crisp inputs can be normalized such as $e_N = eN_1$, and $\dot{e}_N = \dot{e}N_2$

The value of the normalized factors are decided by trial and error method such as, $N_1 = 0.01$ and $N_2 = 0.0011$.

Then, the two normalized distances D_{1N} and D_{2N} are;

$$D_{1N} = D_1 \cdot N_1$$

And $D_{2N} = D_2 \cdot N_2$

The fuzzy variables chosen here for the normalized distances are zero and positive small and the fuzzy variables chosen for the normalized controller gain are zero, positive small and positive big. So, the fuzzy control rules are:

Table 1: Fuzzy Rules

Rules	D_{1N}	D_{2N}	$K_{fuzzy,N}$
1	Z	Z	Z
2	Z	PS	PS
3	PS	Z	PS
4	PS	PS	PB

For easy calculation, the membership function chosen here is symmetrical triangular membership function. The error and the rate of change of error of the control variables are calculated and then, the two perpendicular distances of the actual state from the origin of the phase plane are calculated. These two distances are normalized to the fuzzy domain of universe. For a particular value of the normalized distances, the degrees of membership of these two distances obtained are:

$$\mu_{1PS} = D_{1N} \text{ and } \mu_{1Z} = 1 - D_{1N} \quad (4.1d)$$

and $\mu_{2PS} = D_{2N} \text{ and } \mu_{2Z} = 1 - D_{2N} \quad (4.1e)$

where μ_{1PS} = Degree of membership of D_{1N} in Positive Small set.

μ_{1Z} = Degree of membership of D_{1N} in Zero set.

μ_{2PS} = Degree of membership of D_{2N} in Positive Small set.

μ_{2Z} = Degree of membership of D_{2N} in Zero set.

From the degree of membership of two inputs, the degree of membership of output i.e. the normalized controller gain of the two inputs are calculated as;

Rule 1: $\mu_{KZ} = \mu_{1Z} \wedge \mu_{2Z} = \min(\mu_{1Z}, \mu_{2Z})$

Where μ_{KZ} = degree of membership of output in zero set.

$$\text{Rule 2: } \mu_{KPS1} = \mu_{1Z} \wedge \mu_{2PS} = \min(\mu_{1Z}, \mu_{2PS})$$

Where μ_{KPS1} = degree of membership of output in Positive Small set according to rule 2.

$$\text{Rule 3: } \mu_{KPS2} = \mu_{1PS} \wedge \mu_{2Z} = \min(\mu_{1PS}, \mu_{2Z})$$

Where μ_{KPS2} = degree of membership of output in Positive Small set according to rule 3.

So the resulting degree of membership in Positive Small set is;

$$\mu_{KPS} = \mu_{KPS1} \vee \mu_{KPS2} = \max(\mu_{KPS1}, \mu_{KPS2})$$

$$\text{Rule 4: } \mu_{KPB} = \mu_{1PS} \wedge \mu_{2PS} = \min(\mu_{1PS}, \mu_{2PS})$$

Where μ_{KPB} = degree of membership of output in Positive Big set.

The fuzzy AND (\wedge) operation denotes the minimum of the two quantities. Similarly, the fuzzy OR (\vee) operation denotes the maximum of the two quantities since rule-2 and rule-3 result the same output, so to find the degree of membership of output in the Positive Small set, the OR operation is used.

Let us consider an example with the two normalized distances $D_{1N} = 0.4$ and $D_{2N} = 0.7$

So the degree of membership of the output sets is:

$$\begin{aligned} \mu_{1PS} &= 0.4 \\ \mu_{2PS} &= 0.6 \\ \mu_{1Z} &= 0.7 \\ \mu_{2Z} &= 0.3 \end{aligned}$$

From the fuzzy rule set: $\mu_{KZ} = \min(\mu_{1Z}, \mu_{2Z}) = 0.3$

$$\mu_{KPS1} = \min(\mu_{1Z}, \mu_{2PS}) = 0.6$$

$$\mu_{KPS2} = \min(\mu_{1PS}, \mu_{2Z}) = 0.3$$

$$\mu_{KPS} = \max(\mu_{KPS1}, \mu_{KPS2}) = 0.6$$

$$\mu_{KPB} = \min(\mu_{1PS}, \mu_{2PS}) = 0.4$$

With the above data for the normalized distances, degree of membership of the output set and from the fuzzy rule set, the defuzzified output can be calculated as shown below.

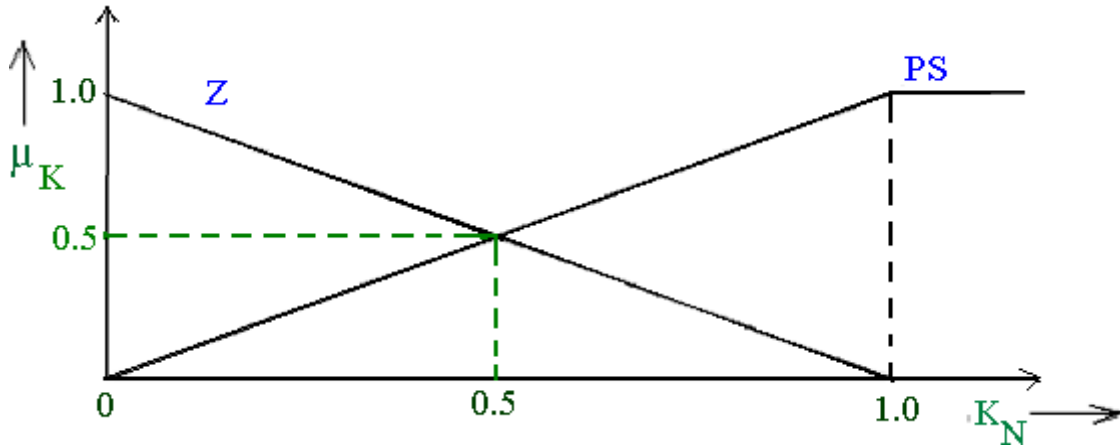


Fig 4.2 Membership functions for normalized inputs

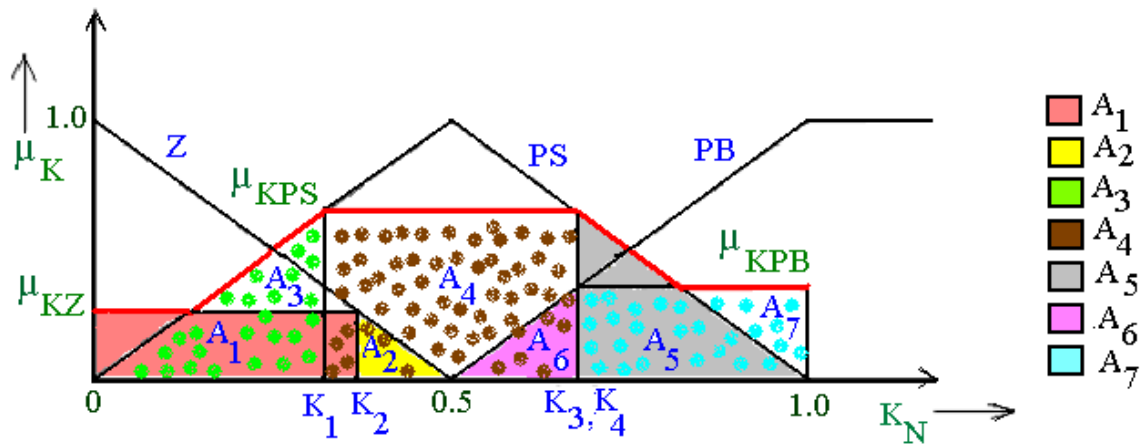


Fig 4.3 Membership functions for the normalized outputs

Fig 4.3 shows the normalized output membership function with the symmetrical triangular membership function for the normalized inputs. This output membership function is divided into areas A_1 , A_2 , A_3 , A_4 , A_5 , A_6 and A_7 . The fuzzy output variables are converted to crisp variables by defuzzification. The method used here for defuzzification is centre of area method (COA).

With this, the defuzzified output of the controller gain is;

$$1.3.1.1 \quad K_{fuzzy,N} = \frac{\int \mu_{out} \cdot K_n \cdot dK_n}{\int \mu_{out} \cdot dK_n} = \frac{\sum I_{num}}{\sum I_{den}} \quad (4.2)$$

From fig 4.3, the integral of the numerator and denominator can be found out for different areas.

Where $\sum I_{num}$ = Integral of the numerator

$\sum I_{den}$ = Integral of the denominator

$$\text{For a rectangular area, } \sum I_{num} = \mu_{out} \cdot \left(\frac{K_H^2 - K_L^2}{2} \right) \quad (4.3a)$$

$$\text{and } \sum I_{den} = \mu_{out} \cdot (K_H - K_L) \quad (4.3b)$$

$$\text{For a triangular area, } \sum I_{num} = \frac{\mu_{out}}{6(K_H - K_L)} (K_H^3 + 2K_L^3 - 3K_H \cdot K_L^2) \quad (4.4a)$$

$$\text{and } \sum I_{den} = \frac{\mu_{out}}{2} \cdot (K_H - K_L) \quad (4.4b)$$

K_H and K_L = Higher limit and lower limit of the fuzzy value of output of each area.

The higher and lower limit of the fuzzy value of output of each area can be obtained from geometry, and by putting the values of the membership functions.

$$K_1 = \frac{\mu_{KPS}}{2} = \frac{0.6}{2} = 0.3; \quad K_2 = \frac{1 - \mu_{KZ}}{2} = \frac{1 - 0.3}{2} = 0.35$$

$$K_3 = \frac{2 - \mu_{KPS}}{2} = \frac{2 - 0.6}{2} = 0.7; \quad K_4 = \frac{1 + \mu_{KPB}}{2} = \frac{1 + 0.4}{2} = 0.7$$

$$\text{For area } \mathbf{A}_1, \quad \sum I_{num1} = \mu_{out} \cdot \frac{K_1^2}{2} = 0.0135$$

$$\sum I_{den1} = \mu_{out} \cdot K_1 = 0.09$$

$$\text{For area } \mathbf{A}_2, \quad \sum I_{num2} = \mu_{out} \cdot \frac{(0.125 + 2K_2^3 - 1.5K_2^2)}{6(0.5 - K_2)} = 9 \times 10^{-3}$$

$$\sum I_{den2} = \mu_{out} \cdot \left(\frac{0.5 - K_2}{2} \right) = 0.0225$$

$$\text{For area } \mathbf{A}_3, \quad \sum I_{num3} = \mu_{out} \cdot \frac{K_1^2}{6} = 9 \times 10^{-3}$$

$$\sum I_{den3} = \mu_{out} \cdot \frac{K_1}{2} = 0.09$$

For area **A₄**,
$$\sum I_{num4} = \mu_{out} \cdot \frac{(K_4^2 - K_1^2)}{2} = 0.12$$

$$\sum I_{den4} = \mu_{out} (K_4 - K_2) = 0.21$$

For area **A₅**,
$$\sum I_{num5} = \mu_{out} \cdot \frac{(1 + 2K_4^3 - 3K_4^2)}{6(1 - K_4)} = 0.072$$

$$\sum I_{den5} = \mu_{out} \frac{(1 - K_4)}{2} = 0.09$$

For area **A₆**,
$$\sum I_{num6} = \mu_{out} \cdot \frac{(K_4^3 - 0.75K_2 + 0.25)}{6(K_4 - 0.5)} = 0.1101$$

$$\sum I_{den6} = \mu_{out} \left(\frac{K_4 - 0.5}{2} \right) = 0.04$$

For area **A₇**,
$$\sum I_{num7} = \mu_{out} \cdot \frac{(1 - K_4^2)}{2} = 0.102$$

$$\sum I_{den7} = \mu_{out} (1 - K_4) = 0.12$$

Now, from eqⁿ (4.2), the defuzzified normalized controller gain is calculated as,

$$K_{fuzzy,N} = \frac{\sum I_{num}}{\sum I_{den}} = \frac{0.4356}{0.6625} = 0.657$$

This defuzzified, but, normalized controller gain can be denormalized by selecting a proper denormalizing factor N .

According to sliding mode control, the controller gain $K = (|\Delta G_{max}| + D_{max} + \eta + \nu)$

Similarly, for fuzzy sliding mode controller, we can get the maximum value of the defuzzified normalized output controller gain such as; $K_{fuzzy,max} \geq (|\Delta G_{max}| + D_{max} + \eta + \nu)$

So, the denormalizing factor is,
$$N = \frac{K_{fuzzy,max}}{K_{fuzzy,N,max}}$$

After different simulation studies, the suitable value of the denormalizing factor is taken equal to 11000.

So, defuzzified denormalized controller gain is;

$$K_{fuzzy,max} = 11000 \times 0.6 = 6600$$

4.5 Simulation Results and Discussions

Case-1: Step change in reference rotor speed

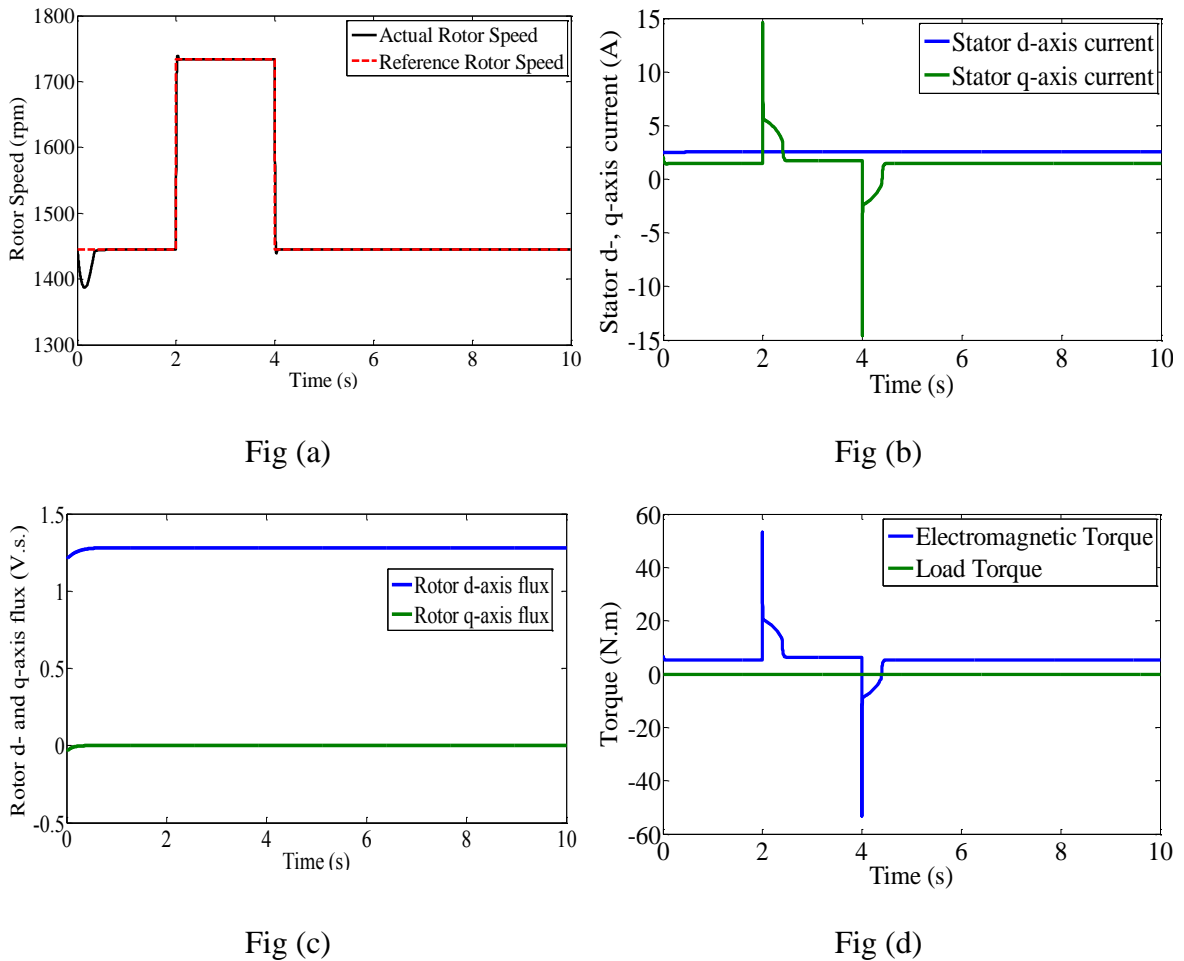


Figure 4.4 Simulation responses during Step Change in Reference Rotor Speed

(a) Reference and actual rotor speed (b) Stator d- and q-axis current (c) Rotor d- and q-axis flux (d) Electromagnetic Torque and Load Torque

The rotor reference speed is stepped from its base value of 1445rpm to 1734rpm between $t = 2s$ to $t = 4s$ i.e. 20% of its base speed. The stator d-axis current remains constant at 2.531A whereas the q-axis stator current undergoes a transient rise of current of magnitude 14.6A for 0.5s at $t = 2s$ and at $t = 4s$. The stator phase-a current also undergoes a transient disturbance due to the step change in rotor speed from 2.915A to a peak value of magnitude of about 6A. The

rotor d-axis flux remains constant at 1.233V.s whereas the rotor q-axis flux remains at zero. The electromagnetic torque developed varies with the variation of stator torque component of current. At no load, the electromagnetic torque developed is 5.296N.m.

Case-2: Trapezoidal change in reference rotor speed

The rotor reference speed is varied in a trapezoidal manner from zero at $t = 0$ to 1734rpm i.e. 20% increase of its base speed. The actual rotor speed follows the reference rotor speed. The torque component of current varies with the variation of rotor reference speed. With the rotor speed remaining constant between $t = 1$ s to $t = 4$ s, the stator d-axis current remains constant at 2.53A and the stator q-axis current varies with the variation of rotor speed and thus the electromagnetic torque with load torque zero. During forward motoring mode, the torque component of stator current is 1.744A and with the reversal of speed, the current also reverses. During reverse motoring mode, the q-axis current is having a magnitude of 1.744A. A stator q-axis voltage of 501V is produced and it varies with the variation of rotor speed. With the reversal of rotor speed, the q-axis stator voltage reverses and a voltage of magnitude 051V is produces during reverse motoring mode. The stator phase-a current undergoes a transient disturbance during the change of rotor speed and have a steady state value of 3.07A.

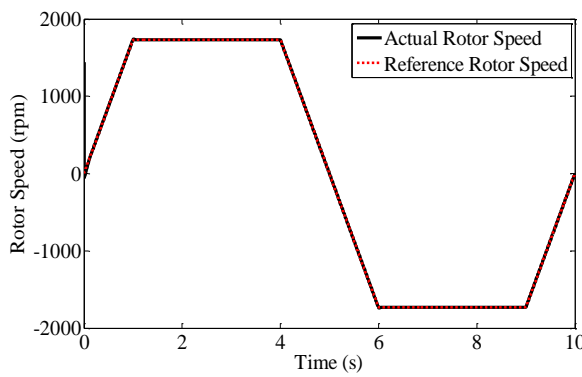


Fig (a)

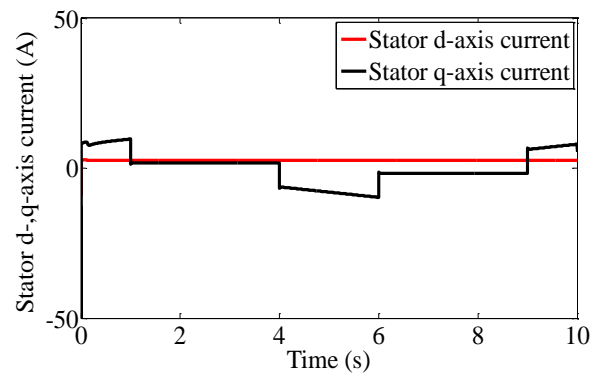


Fig (b)

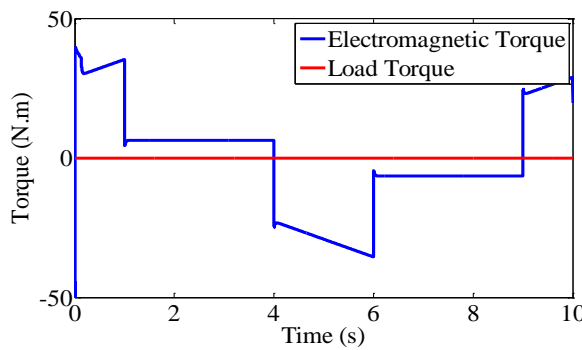


Fig (c)

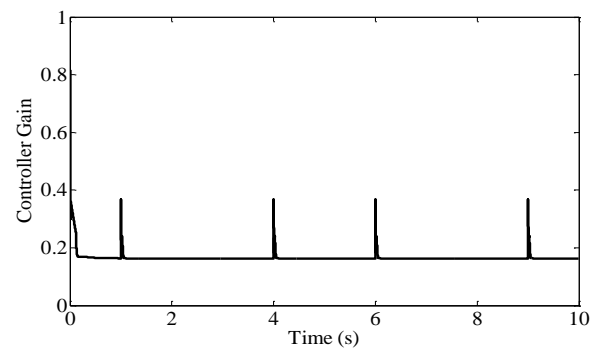


Fig (d)

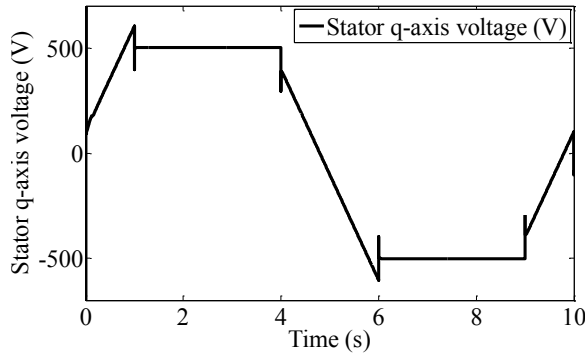


Fig (e)

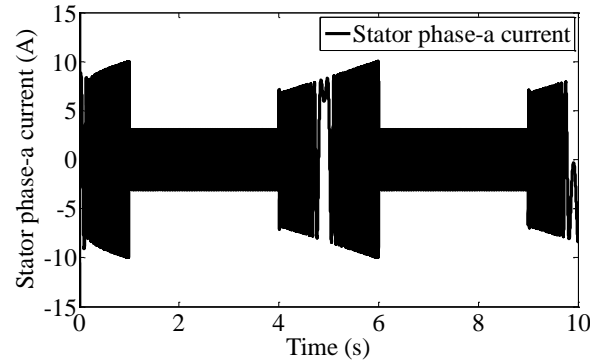


Fig (f)

Figure 4.5 Simulation responses during Trapezoidal Change in Reference Rotor Speed

(a) Reference and actual rotor speed (b) Stator d- and q-axis current (c) Electromagnetic Torque and Load Torque (d) Controller Gain (e) Stator q-axis voltage (f) Stator phase-a current

Case-3: Flux weakening mode

With the increase in rotor speed above the base speed results in flux weakening mode. The rotor rotates at a speed greater than 20% of its base speed i.e. at 1734rpm and the rotor d-axis flux is observed. In the flux weakening mode, the rotor d-axis flux decreases from its constant value of 1.233V.s to 1.037V.s. This is known as flux weakening mode where the rotor flux varies inversely as the rotor speed increases. The q-axis rotor flux remains constant at zero. The rotor rotates at an increased speed of 1734rpm from $t = 2s$ to $t = 4s$ and then decreases to its original value. It is observed that due to the change in rotor flux, the flux component of stator current decreases from 2.53A to 2.073A from $t = 2s$ to $t = 4s$ weakens and then returns to its original value as the rotor speed decreases to its base speed. The stator q-axis current, being the function of rotor speed, varies with the change in rotor speed. With a step increase of rotor speed, the torque component of stator current increases from 1.744A to 2.168A after a transient disturbance of 0.4s. The rotor d- and q-axis flux plot is shown below.

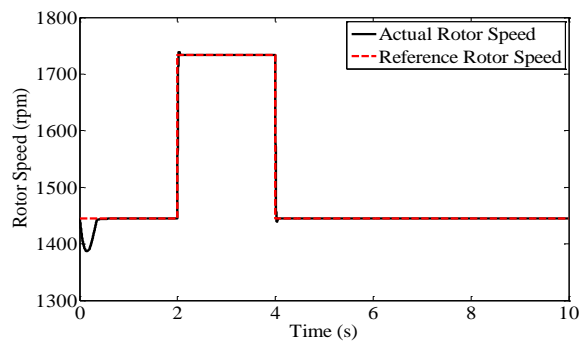


Fig (a)

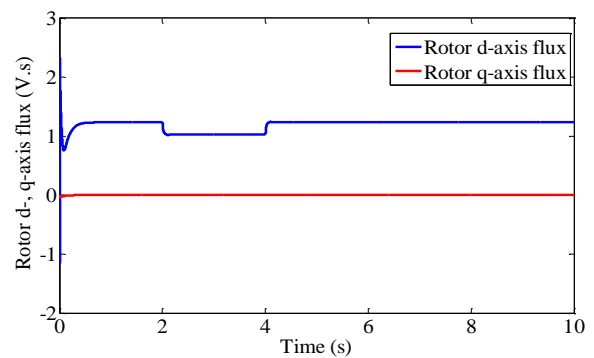


Fig (b)

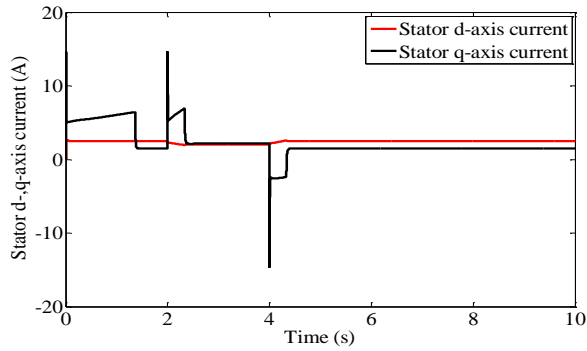


Fig (c)

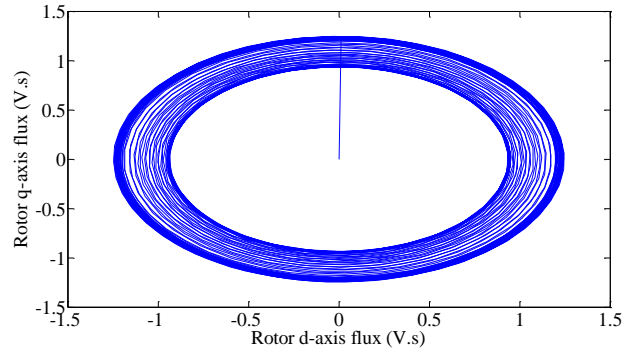


Fig (d)

Figure 4.6 Simulation responses during flux weakening mode

- (a) Reference and actual rotor speed (b) Rotor d- and q-axis flux (c) Stator d- and q-axis current (d) Rotor d-axis vs. rotor q-axis flux plot

Case-4: Step change in load torque

The rotor reference speed is varied in a trapezoidal manner from zero to 1734rpm from $t = 0$ to $t = 1$ s. The speed decreases from 1734rpm i.e. from forward motoring mode to forward generating mode. The load torque is varied from zero to the rated load torque of 24N.m in forward motoring mode and then from zero to -24N.m in reverse motoring mode. With the variation of load torque, the flux component of stator current remains constant whereas the torque component of stator current increases from 5.483A to 30.5A. The rotor speed decreases from 1734rpm to rpm. The stator phase-current increases from 6.6A to 31A with the increase of load and with the variation of rotor speed. The no load electromagnetic torque increases from 6.35N.m to 30.35n.m due to the applied load between $t = 2$ s to $t = 3$ s.

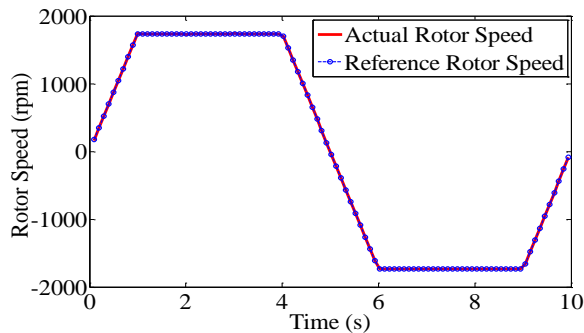


Fig (a)

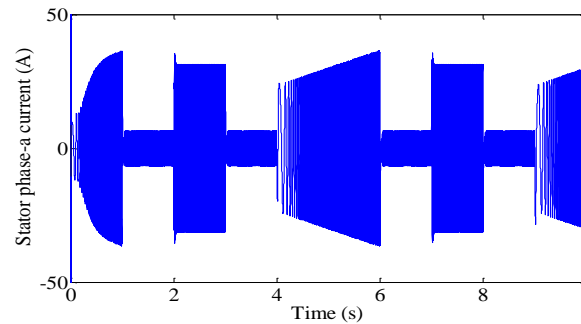


Fig (b)

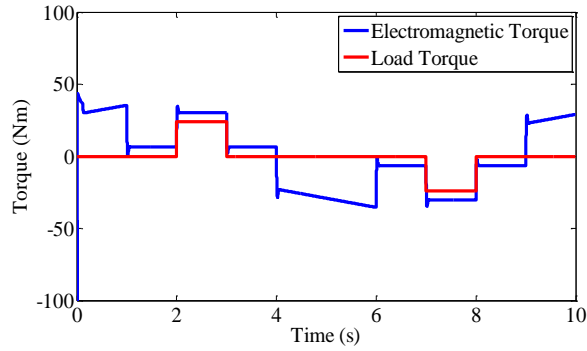


Fig (c)

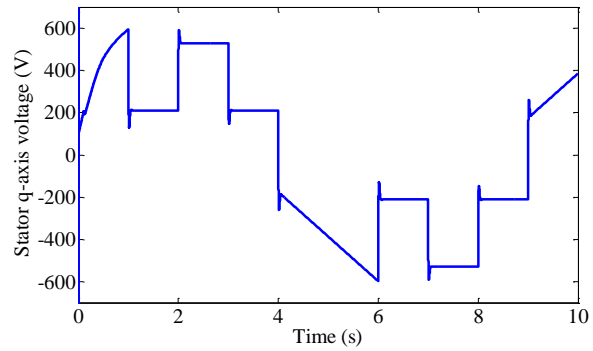


Fig (d)

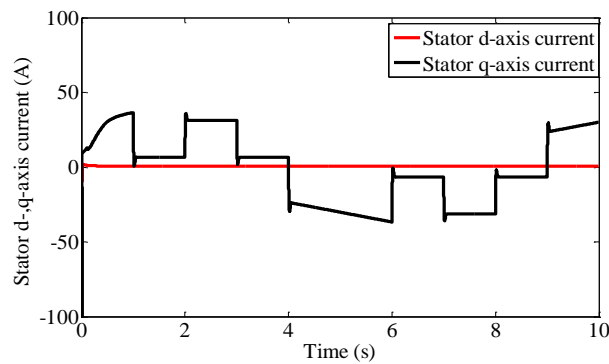


Fig (f)

Figure 4.7 Simulation responses due to change of load torque

(a) Reference and actual rotor speed (b) Stator d- and q-axis current (c) Electromagnetic torque and load torque (d) Stator q-axis voltage (e) Controller gain (f) Stator d- and q-axis current

Case – 4: Parameter Variations

As the rotor starts to rotate, with the increase in rotor speed, the temperature increases. So, the induction motor parameters such as stator and rotor resistance start to vary. With the variation of load torque also, the nature of various responses of the stator and rotor dependent parameters is studied. The robustness of the fuzzy sliding mode controller is verified. During the transient period of $t = 0$ to $t = 2s$, the rotor resistance remains constant. After $t = 2s$, with the linear increase in rotor speed and with the passage of time, the rotor resistance increases from 5.46Ω to 30Ω . So, the rotor resistance becomes 5.5 times the actual rotor resistance and the responses of the induction motor are observed. Also, after $t = 2s$, the stator resistance increases from its actual value of 7.34Ω to 11.008Ω i.e. about 1.5 times its actual value with the increase in temperature.

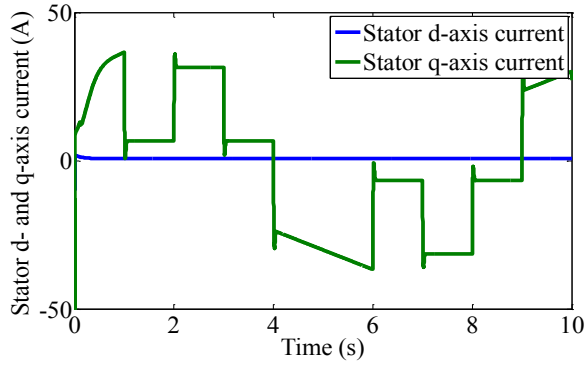


Fig (g)

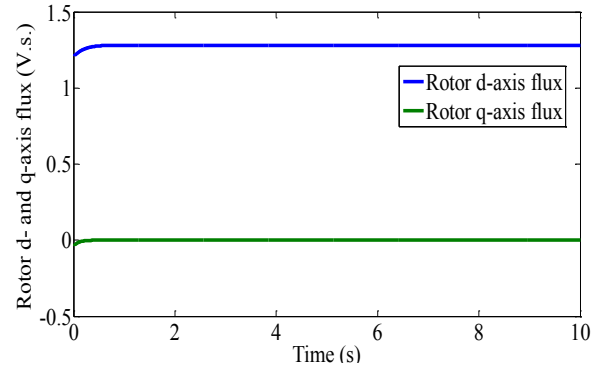


Fig (h)

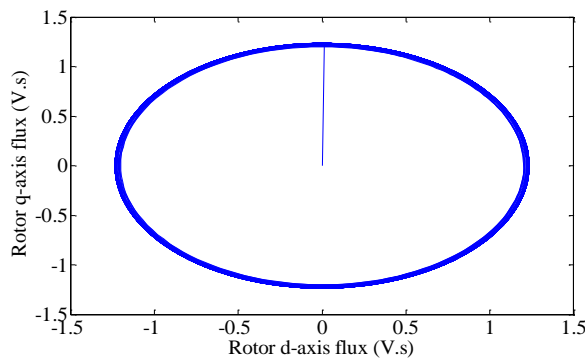


Fig (i)

Figure 4.8 Simulation responses due to Parameter Variations

(a) Reference and actual rotor speed (b) Rotor resistance and Stator resistance (c) Stator phase-a current (d) Electromagnetic torque and load torque (e) Stator q-axis voltage (f) Controller gain (g) Stator d- and q-axis current (h) Rotor d- and q-axis flux (i) Rotor d-axis vs. rotor q-axis flux plot

4.6 Conclusion

The induction motor is modeled and the fuzzy sliding mode controller with estimation in system dynamics is designed. The block diagram of the fuzzy sliding mode controller is shown in fig 4.1. The two normalization factors are selected from the repeated simulation. The fuzzy variables are selected at random and the fuzzy sliding mode controller is designed by taking triangular symmetrical membership function. The centre of area method is used for the defuzzification purpose. The simulation is done and its robustness is verified under the conditions of step and trapezoidal change of speed, variation of load torque, in flux weakening

mode and with motor parameter variation. The system responses are observed, studied and it is obtained that irrespective of the variation of induction motor parameters, the fuzzy sliding mode controller gives satisfactory performance. Also, the fuzzy sliding mode control technique is faster than the sliding mode control with boundary layer.

CHAPTER – 5
CONCLUSION

5 Conclusion

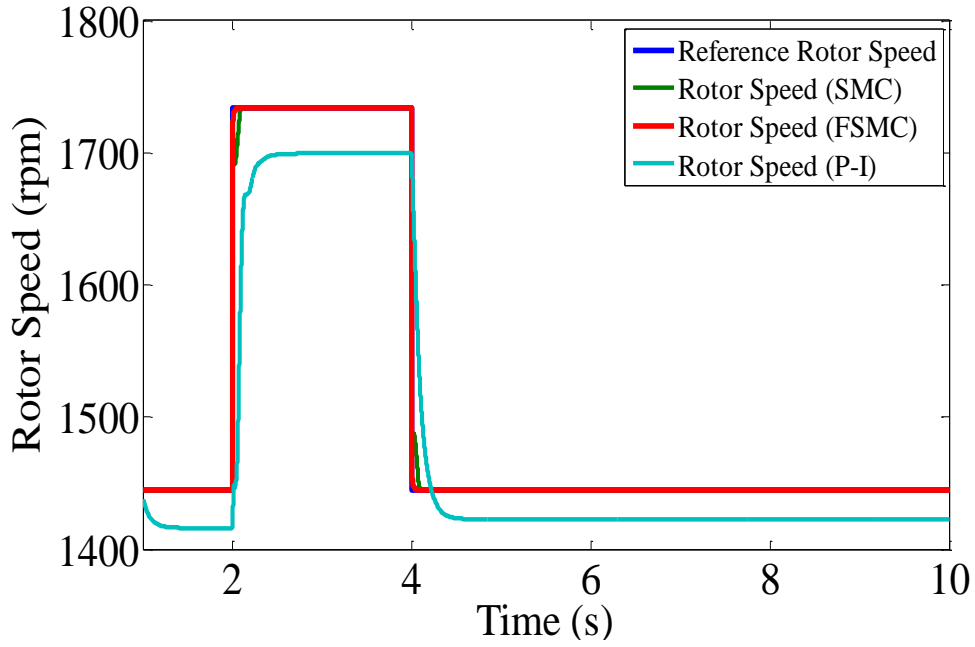
The vector control of induction motor using linear and nonlinear controllers, rotor flux estimation using voltage model based estimation and rotor speed estimation scheme is discussed for an inverter fed induction motor drive. A comparison of the controller schemes is made which is tabulated below. The comparison of all the responses such as stator d- and q-axis voltages, stator q-axis current, and rotor speed variation with step change in reference speed as well as with trapezoidal variation of rotor speed with load torque applied and the variation of electromagnetic torque with load torque variation is shown below in individual plates. The assessment of the work is discussed here along with the future scope of the research.

5.1 Assessment of The Work

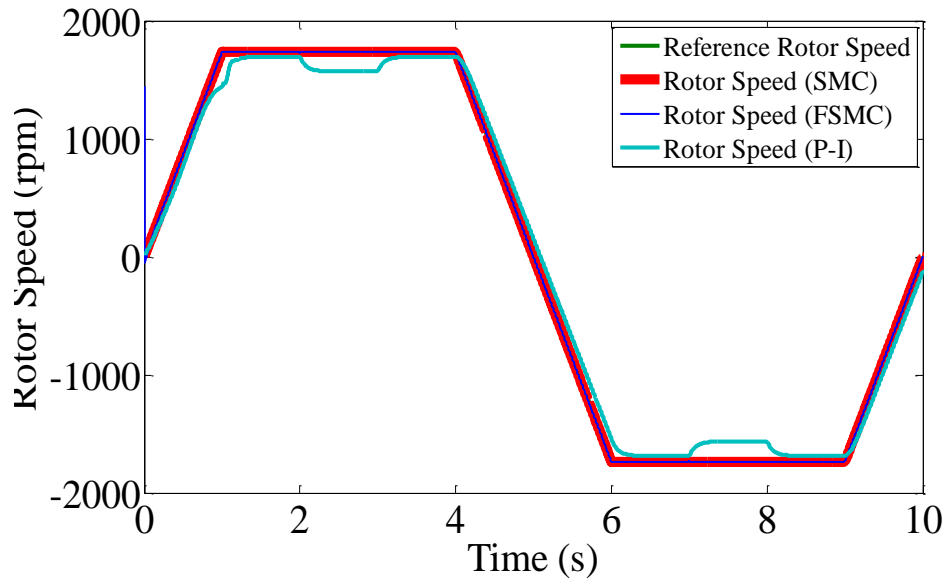
- ❖ A nonlinear dynamic model of the induction motor is mathematically modeled in synchronously rotating reference frame. The simulation is done with the synchronously rotating reference frame.
- ❖ The induction motor is linearized into two subsystems i.e. electrical and mechanical subsystem. The P-I controller is designed to determine the gains of the controller using pole-zero cancellation method. The vector control of induction motor is simulated using P-I controller and the responses are studied using both load torque and speed variation and machine parameters variation.
- ❖ The induction motor responses are improved using sliding mode controller and the simulation is done using different circumstances. The rotor speed is estimated using direct synthesis of state equation to make it sensorless.
- ❖ To overcome the disadvantages of sliding mode controller such as chattering and high controller gain, the fuzzy sliding mode controller is used for the simulation of vector controlled induction motor drive.

5.2 A comparison of the responses of P-I, SMC and FSMC:

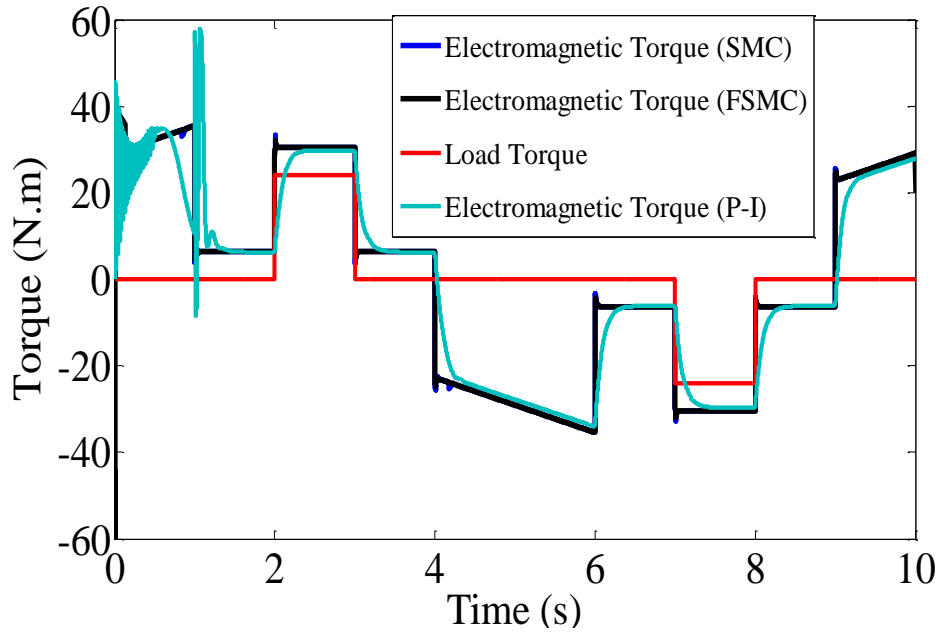
Case-1: Time responses of rotor speed with step change in reference rotor speed:



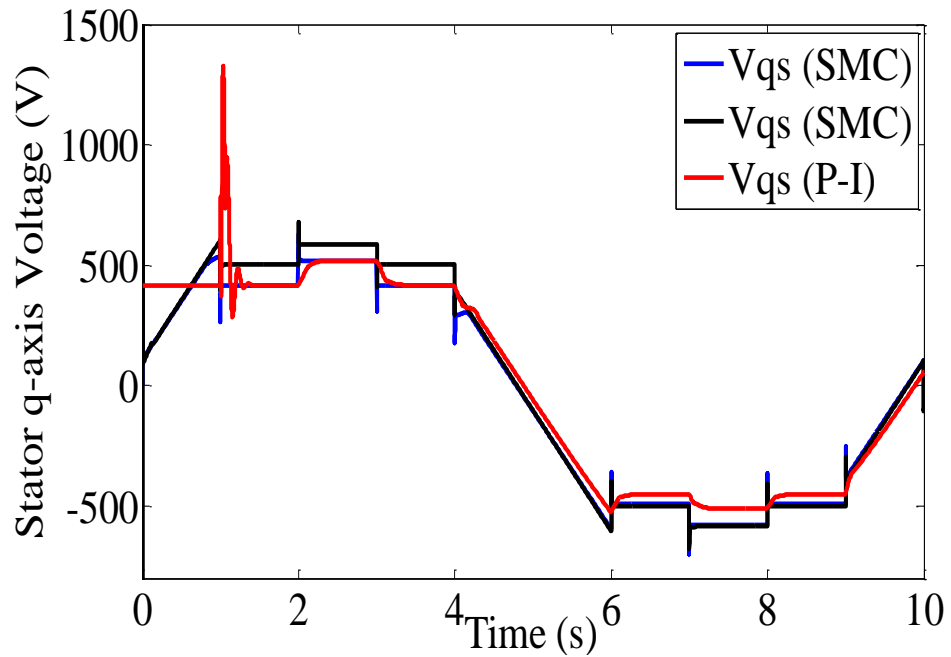
Case-2: Time responses of rotor speed with trapezoidal change in reference rotor speed with load torque applied:



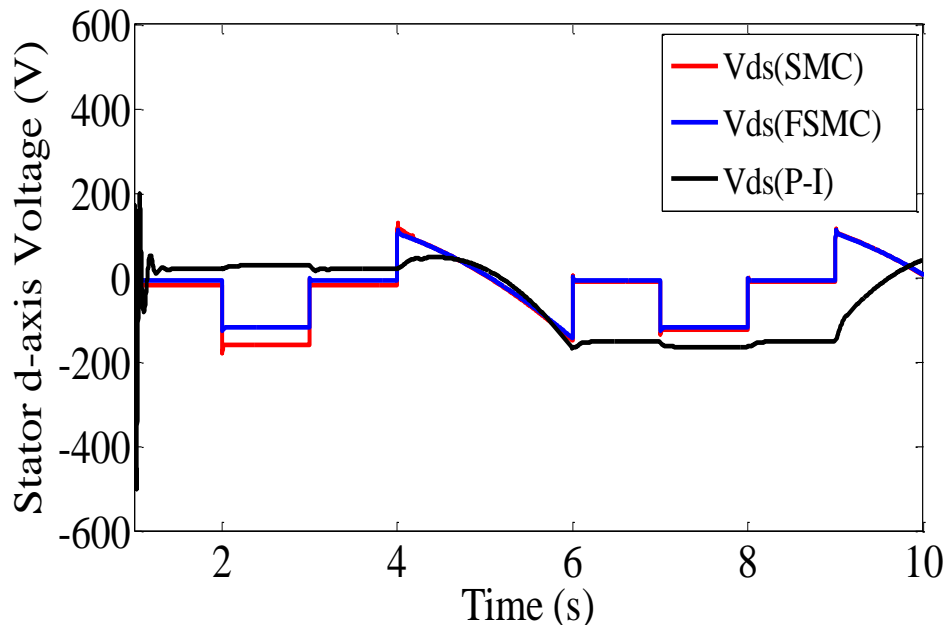
Case-3: Time responses of electromagnetic torque with change in load torque applied:



Case-4: Time response of stator q-axis voltage with trapezoidal change in speed:



Case- 5: Time response of stator d-axis voltage with trapezoidal change in rotor speed with load torque applied:



Case- 6: Time response of stator d-axis current with trapezoidal change in rotor speed with load torque applied:

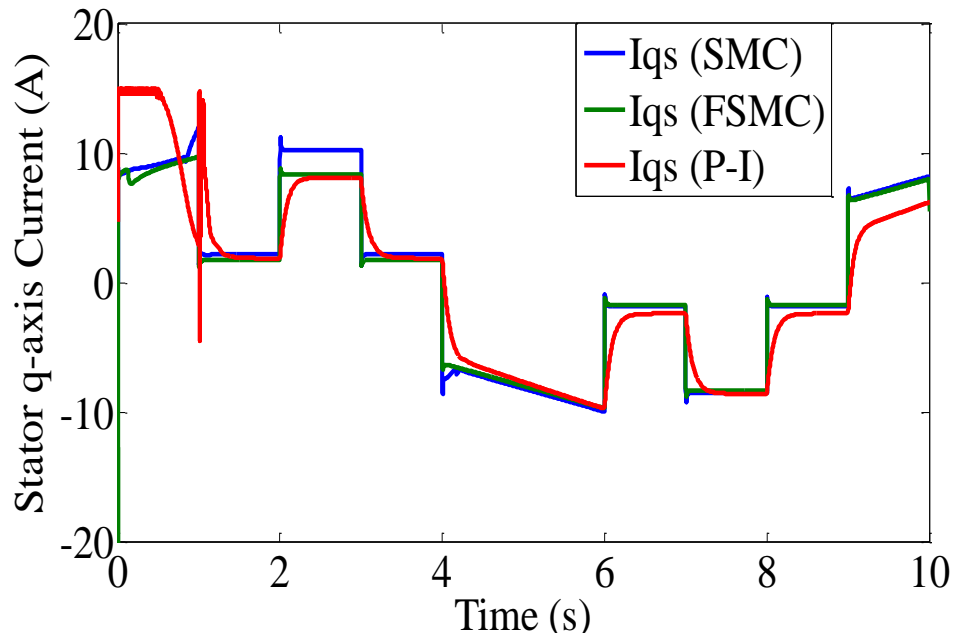


Table -2: Performance comparison of the controllers for a step change in rotor speed from 1445rpm to 1734rpm

Type of Controller	Settling Time of rotor speed in sec.	% Overshoot in I_{as}	% Overshoot in i_q
P-I controller	0.25	88.08	93.24
Sliding mode controller	0.045	58.27	89.72
Fuzzy sliding mode controller	0.201	62.06	60

Table – 3: Performance comparison of the controllers for a step change in load torque from 0 to 24Nm

Type of Controller	% drop in rotor speed	Settling Time of rotor speed in sec.
P-I controller	2.3	0.4
Sliding mode controller	0.05	0.2
Fuzzy sliding mode controller	0.34	0.34

Table – 4: Performance comparison of the controllers for flux weakening mode

Type of Controller	Settling Time of rotor flux in sec.
P-I controller	0.4
Sliding mode controller	0.2
Fuzzy sliding mode controller	0.25

5.3 Scope For The Future Work

- ❖ For future work, the induction motor can be modeled using magnetic saturation. The direct torque control strategy with different nonlinear hybrid controllers can be used for induction motor control for its performance improvement.
- ❖ The rotor speed and flux can be estimated by online parameter estimation techniques in order to observe the effects of motor parameters during operating conditions. Different methods based on adaptive systems, Kalman filter, extended Kalman filter, estimators based on neural networks can be used to improve the estimation accuracy.
- ❖ The value of motor parameters such as stator and rotor resistances can be estimated to know their exact value with respect to temperature variation.

References

- [1] B. K. Bose “*Modern Power Electronics and AC Drives*” Prentice-Hall Publication, New Delhi, 2008.
- [2] A. M., Trzynadlowski “*Control of Induction Motor*” Academic Press, London, 2001.
- [3] P. Vas, “*Sensorless Vector and Direct Torque Control*”, New York: Oxford Science, 1998.
- [4] W. L. Erdman and R. G. Hoft, “*Induction machine field orientation along air gap and stator flux,*” IEEE Trans. On Energy Conversion, vol. 5, no. 1, Mar,1990, pp.115-12.
- [5] E. Y. Ho and P. C. Sen, “*Decoupling control of Induction Motor Drives*”, IEEE Proc., vol. 35, no. 2, May 1988,pp. 253-262.
- [6] S. Sathiakumar, S. K. Biswas, and J. Vithyathil, “*Microprocessor based field-oriented control of a CSI-fed induction motor drive,*” IEEE Trans. on Industrial Electronics, vol. 33, Feb. 1986, pp. 39-43.
- [7] T. M. Rowan and R. J. Kerkman, “*A new synchronous current regulator and analysis of current regulated PWM inverters,*” IEEE Trans. on Ind. Appl., vol. 22, no. 4, Jul/Aug. 1986, pp. 678-690.
- [8] H. Nagase, Y. Matsue, K. Ohnisi, H. Ninomiya and T. koike, “*High performance induction motor drive system using a PWM inverter,*” IEEE Trans. on Ond. Appl., vol. 20, no. 6, 1984, pp. 1482-1489.
- [9] M. Vélez-Reyes and G. C. Verghese, “*Decomposed algorithms for speed and parameter estimation in induction machines,*” IFAC Symposium on Non-linear Control System Design, Bordeaux, France, 1992.
- [10] M. Vélez-Reyes, K Minami, G. C. Verghese, “*Recursive speed and parameter estimation for induction machines,*” IEEE Ind. Applicat. Society Meeting, San Diego, 1989.
- [11] M. Bodson and J. Chiasson, “*A comparison of sensorless speed estimation methods for induction motor control,*” Proc ACC, Anchorage, AK May.2002, pp. 3076-3081.
- [12] Y. R. Kim, S. K. Sul, and M. H. Park, “*Speed sensorless vector control of induction motor using extended Kalman filter,*” IEEE Trans. on Ind. Appl., vol. 30, no. 5, 1994, pp. 1225-1233.
- [13] F.Z.Peng, T.Fukao “*Robust Speed Identification for Speed Sensorless Vector Control of Induction Motors*” IEEE Tran. IA vol. 30, no. 5, pp.1234-1239, Oct.1994.

- [14] C.Schauder “*Adaptive Speed Identification for Vector Control of Induction Motor without Rotational Transducers*” IEEE Tran. on Ind. Appl., vol. 28, no. 5, pp. 1054-1061,Oct.1992.
- [15] A. Mohamed,A. G. Aissaoui,Y. Ramdani, A. K. Zeblah, “*Sliding mode speed and flux control of field-oriented induction machine*”, Acta Electrotechnica et Informatica no. 1, vol. 7, 2007.
- [16] K Minami, M. Vélez-Reyes, D. Elten, G. C. Verghese and D. Filbert, “*Multistage speed and parameter estimation for induction machines,*” IEEE Power Electronics Specialist’s Conference, Boston MA, Jun. 1991.
- [17] M. Vélez-Reyes and G. C. Verghese, “*Decomposed algorithms for speed and parameter estimation in induction machines,*” IFAC Symposium on Non-linear Control System Design, Bordeaux, France, 1992.
- [18] M. Vélez-Reyes, K Minami, G. C. Verghese, “*Recursive speed and parameter estimation for induction machines,*” IEEE Ind. Applicat. Society Meeting, San Diego, 1989.
- [19] M. Bodson and J. Chiasson, “*A comparision of sensorless speed estimation methods for induction motor control,*” Proc ACC, Anchorage, AK May,2002, pp. 3076-3081.
- [20] F.Z.Peng, T.Fukao “*Robust Speed Identification for Speed Sensorless Vector Control of Induction Motors*” IEEE Trans. IA vol. 30, no. 5, pp.1234-1239, Oct.1994.
- [21] C.Schauder “*Adaptive Speed Identification for Vector Control of Induction Motor without Rotational Transducers*” IEEE Tran. on Ind. Appl., vol. 28, no. 5, pp. 1054-1061,Oct.1992.
- [22] C. C. Chan and H. Q. Wang, “*New scheme of sliding mode control for high performance induction motor drives,*” IEEE proc. On Electric Power Applications, vol. 143, no. 3, May 1996, pp. 177-185

Conference Paper Published:

1. Swetananda Jena, Kanungo Barada Mohanty, “Robust field oriented induction machine control using SMC,” 5th PSU-UNS International Conf. on ICET, Phuket, Thailand, May 2011.
2. Swetananda Jena, Kanungo Barada Mohanty, “Robust Sensorless field oriented control using sliding mode,” IEEE Conference, Hyderabad, Dec 2011.

Specifications and Parameters of the Machine

Induction Motor: Three phase, 3-Phase, squirrel cage induction motor, 5HP (3.7kW), 50Hz,
4 pole, 415V, 1445rpm,

Table 5: Parameters of the Induction Motor

Sl. No.	Nominal per phase parameters referred to stator	Values in SI units
1	Stator Resistance (R_s)	7.34 Ω
2	Rotor Resistance (R_r)	5.46 Ω
3	Mutual Inductance (L_m)	0.5 H
4	Stator self Inductance (L_s)	0.521 H
5	Rotor self Inductance (L_r)	0.521H
6	Moment of Inertia (J)	0.16 kg-m ²
7	Damping Co-efficient (B)	0.035 N.m.s/rad

Table 6: Values of the Parameters used in the Induction Motor Model

a_1	a_2	a_3	a_4	a_5
300.51	244.405	23.3226	10.48	5.24